

Evolutionary Retrofitting

MATHURIN VIDEAU, Meta AI, France and TAU, INRIA and LISN (CNRS & Univ. Paris-Saclay), France

MARIIA ZAMESHINA, Univ Gustave Eiffel, CNRS, LIGM, France and Meta AI, France

ALESSANDRO LEITE, INSA Rouen Normandy, University of Rouen Normandy, LITIS UR 4108, France

LAURENT NAJMAN, Univ Gustave Eiffel, CNRS, LIGM, France and Department of Mathematics - Khalifa University, UAE

MARC SCHOENAUER, TAU, INRIA and LISN (CNRS & Univ. Paris-Saclay), France

OLIVIER TEYTAUD, Thales - CortAix-Labs, France

AfterLearnER (After Learning Evolutionary Retrofitting) consists in applying evolutionary optimization to refine fully trained machine learning models by optimizing a set of carefully chosen parameters or hyperparameters of the model, with respect to some actual, exact, and hence possibly non-differentiable error signal, performed on a subset of the standard validation set. The efficiency of AfterLearnER is demonstrated by tackling non-differentiable signals such as threshold-based criteria in depth sensing, the word error rate in speech re-synthesis, the number of kills per life at Doom, computational accuracy or BLEU in code translation, image quality in 3D generative adversarial networks (GANs), and user feedback in image generation via Latent Diffusion Models (LDM). This retrofitting can be done after training, or dynamically at inference time by taking into account the user feedback. The advantages of AfterLearnER are its versatility, the possibility to use non-differentiable feedback, including human evaluations (i.e., no gradient is needed), the limited overfitting supported by a theoretical study, and its anytime behavior. Last but not least, AfterLearnER requires only a small amount of feedback, i.e., a few dozen to a few hundred scalars, compared to the tens of thousands needed in most related published works.

Additional Key Words and Phrases: Evolutionary algorithms, machine learning, speech synthesis, hyperparameters

1 INTRODUCTION

Retrofitting is the addition of new technology or features to older systems [Dawson 2007; Dixon and Eames 2013; Douglas 2006]. Retrofitting is routinely used in industry, e.g., in the building sector, to adapt old buildings to new needs or new regulations. When it comes to machine learning models, the term is mainly used in natural language processing (NLP) since the seminal work of Faruqi et al. [2015a], who modified the representation of the word vector to take into account some semantic knowledge. This is done in a *post hoc* way, i.e., without retraining the whole network, though nevertheless requiring a differentiable auxiliary loss function (more in Section 2.1.3).

Other examples of such retrofitting (though not using that term) are used for transfer learning when only some of the last layers of a deep neural network that had been trained for a given task are fine-tuned for another one [Oquab et al. 2023] (more in Section 2.1.1). However, even though they do not involve the whole set of weights, such re-trainings use gradient descent and, therefore, only work with differentiable losses.

On the opposite, gradient-free (aka black-box) optimization offers two main advantages: it does not require the computation of the gradient, thus decreasing the computational cost and memory requirements; and it can handle non-differentiable functions that are out of reach of

Authors' addresses: [Mathurin Videau](#), Meta AI, Paris, France and TAU, INRIA and LISN (CNRS & Univ. Paris-Saclay), Orsay, France, mvideau@meta.com; [Mariia Zameshina](#), Univ Gustave Eiffel, CNRS, LIGM, Champs-sur-Marne, France and Meta AI, Paris, France, mzameshina@gmail.com; [Alessandro Leite](#), INSA Rouen Normandy, University of Rouen Normandy, LITIS UR 4108, Rouen, France, aleite@insa-rouen.fr; [Laurent Najman](#), Univ Gustave Eiffel, CNRS, LIGM, Champs-sur-Marne, France and Department of Mathematics - Khalifa University, Abu Dhabi, UAE, laurent.najman@esiee.fr; [Marc Schoenauer](#), TAU, INRIA and LISN (CNRS & Univ. Paris-Saclay), Orsay, France, marc.schoenauer@inria.fr; [Olivier Teytaud](#), Thales - CortAix-Labs, Palaiseau, France.

gradient-based methods. Indeed, there are many situations where the actual goal of the ML model is better expressed as a non-differentiable metric, and the differentiable metric used for training with stochastic gradient descent (SGD) approaches is only a proxy of such an actual goal. Examples of such situations will be given in Section 5, like e.g., the number of kills in the Doom video game (Section 5.3).

However, black-box optimizers generally do not scale very well with the number of variables, and cannot be used to optimize a large set of parameters (e.g., the weights) of current deep models – with some significant exceptions like, for instance, OpenAI Evolution Strategies [Salimans et al. 2017].

With this in mind, this work proposes AfterLearnER, for *After Learning Evolutionary Retrofitting*, which optimizes in a post-hoc way a small set of parameters and/or hyperparameters of a fully trained model, referred to in the following as the **N-parameters**¹. AfterLearnER is agnostic with respect to the learning algorithm used to train the model. Furthermore, it can optimize any specific loss function, here termed the **N-loss**, that can be different from the one used during the model training. Notably, AfterLearnER can handle non-differentiable **N-losses**, allowing for better alignment with the actual goals of the learning task without the need to run any gradient backpropagation cycle. A detailed presentation of AfterLearnER is given in Section 3.1.

AfterLearnER clearly relates to hyperparameter optimization (HPO) [Feurer and Hutter 2019], transfer learning [Zhuang et al. 2021], and fine-tuning [Lialin et al. 2023] approaches. Furthermore, because AfterLearnER operates after the standard training process, it semantically relates to a number of test-time adaptation (TTA) approaches [Chen et al. 2022; Niu et al. 2022]. The crucial difference from most of these works is that AfterLearnER can handle non-differentiable **N-losses**. AfterLearnER can also be used to handle distributional data shift (like TTA approaches [Niu et al. 2022]) or to adapt the pre-trained model to new tasks, like transfer learning [Oquab et al. 2023], though it is initially conceived to improve the pre-trained model for the same task, the **N-loss** providing a different point of view on that task. These issues are discussed in more detail in Section 2 below and illustrated by the experiments presented in Section 5.

Contributions. The main contributions of this work are as follows:

- We propose **AfterLearnER** (After Learning Evolutionary Retrofitting), a novel gradient-free optimization framework that enables the post-hoc tuning of a small set of parameters or hyperparameters (**N-parameters**) of fully trained machine learning models, using arbitrary target objectives, including non-differentiable loss functions (**N-losses**), without requiring gradient computation or backpropagation.
- In contrast to conventional **fine-tuning**, **transfer learning**, and **test-time adaptation** approaches, which rely on differentiable surrogate losses and retraining cycles, AfterLearnER operates entirely in a black-box optimization setting and can directly optimize the actual performance metrics of interest, even when they are non-differentiable or hard to model.
- We show that AfterLearnER is **training** and **model-agnostic**, and can be seamlessly applied across a wide range of application domains and modalities. We report experimental results in both offline and online settings, including depth estimation, speech re-synthesis, reinforcement learning for video games, code translation, 3D generative modeling, and text-to-image diffusion.
- We provide extensive experimental evidence that AfterLearnER can significantly improve the alignment of a model with real-world target metrics, even when those metrics are not accessible via gradient-based optimization, thus broadening the scope of practical retrofitting

¹We use the singular (**N-parameter**) to denote the full set of parameters or hyperparameters optimized by AfterLearnER.

Table 1. Comparison between different works related to AfterLearnER. The columns from left to right are: Whether their target task is the same as the one used during pre-training; Whether any additional knowledge is needed for the optimization; What proportion of the model parameters are modified; Whether some gradient is needed or not; The number of full backprop optimization that is performed (if any) after the pre-training; The corresponding typical references (there are dozens of other works, and we cannot pretend to be exhaustive).

Framework	Final task	Additional knowledge	Reoptimized parameters	Gradient needed	Additional Full Backprop	References
Hyperparameter tuning	Same	–	Small part	No (outer loop)	Many	<1>
Fine-tuning	Different	Smaller dataset	Depends	Yes	A few	<2>
Transfer learning	Different	Distinct dataset	Entire net	Yes	A few	<3><7>
Test-Time Training	Same	–	Large part	Yes	A few	<4>
Test-Time Adaptation	Same	–	Small part	Yes	None	<5>
Retrofitting	Same	High-level info	Small part	Depends	None	<6>
AfterLearnER	Same	Coarse grain info	Small part or latent vars	No (possibly interactive)	None	

<1> Feurer and Hutter [2019]

<2> Lialin et al. [2023]

<3> Zhuang et al. [2021]

<4> Sun et al. [2020]

<5> Wang et al. [2021]

<6> Faruqui et al. [2015b]

<7> Soemers et al. [2023]

beyond what is achievable with conventional fine-tuning, transfer learning, or test-time adaptation approaches.

The paper is organized as follows. Section 2 surveys the related works: Section 2.1 (resp. Section 2.2) discusses differentiable (resp. non-differentiable) losses, and Section 2.3 introduces the black-box optimization algorithms used in AfterLearnER. Section 3 presents AfterLearnER in detail, following some kind of “user guide” format. Section 3.3 discusses a priori the advantages of the proposed methodology. Section 4 presents our experimental setup and Section 5 presents the experimental results obtained across various applications by AfterLearnER in offline mode for Depth sensing (Section 5.1), speech re-synthesis (Section 5.2), reinforcement learning for Doom video-game (Section 5.3), and code translation (Section 5.4); and by AfterLearnER in online mode for interactive GANs (Section 6.1), 3D-GANs (Section 6.2), and text-to-image (Sections 6.3 and 6.4). Finally, Section 7 globally discusses the results, and Section 8 concludes the paper.

2 RELATED WORK

AfterLearnER is related to a number of previous works, with some significant differences that are summarized in Table 1 along different axes and discussed in turn in this section. We are aware that many other works could have been cited here. However, we did our best to cover the most prominent lines of related work, even if we did not cite all relevant papers in each subsection below to avoid bloating.

We first survey approaches optimizing a differentiable loss before moving on to those that handle non-differentiable losses. And because the latter is the context of AfterLearnER, Section 2.3 then briefly describes black-box optimization tools, focusing on the ones used in the present work.

2.1 Differentiable loss functions

The works below require a differentiable loss function – a critical difference with AfterLearnER.

2.1.1 Fine-tuning and transfer learning. Fine-tuning amounts to optimizing some weights (generally a few layers) of a trained neural network to improve its accuracy for some more specific task than the one it was trained on. Fine-tuning has now become a routine process in deep learning [Lialin et al. 2023]. It is used, for instance, to specialize general-purpose Large Language Models (LLMs) for

downstream tasks [Ouyang et al. 2022], including supervised learning and Reinforcement Learning from Human Feedback (see Section 2.2.1 below). Still, in the context of LLMs, it can be used to “improve” the outcomes of the model following the programmer’s preferences [Rozado 2023]. In such situations, the whole model is fine-tuned using standard gradient-based optimization of the training loss itself, and even though only a fraction of the iterations is needed, this still has a significant cost.

Another use of fine-tuning relates to transfer learning [Zhuang et al. 2021]: a model that has been trained for a specific task can be fine-tuned to perform a different but similar task, freezing most of the model, and optimizing only a fraction of it (e.g., one or a few last layers). Under some mild hypotheses, it has been demonstrated [Giannou et al. 2023; Lu et al. 2022] and later proved [Burkholz 2024] that normalization layers are indeed good candidates for such fine-tuning. This approach is sometimes referred to as Feature Extraction: the frozen layers de facto become feature extractors. Still, the number of unfrozen weights (the \mathfrak{N} -parameter here) can be rather high (e.g., more than 100,000 in [Lu et al. 2022]). Furthermore, here again, a few iterations of the full backprop optimization are needed: The optimization is thus costly, both in computation and in memory.

To mitigate the cost of fine-tuning, Parameter Efficient Fine-Tuning (PEFT) strategies have been developed. A common PEFT approach involves adding a few new blocks to the model, initialized as identity functions while freezing all existing weights, as demonstrated by Houlsby et al. [2019]. These newly introduced parameters allow the model to specialize for new tasks. Another PEFT approach injects trainable low-rank decomposition matrices into each layer of the model [Hu et al. 2021; Liu et al. 2024]. These matrices adapt the model to the new task, making PEFT a practical alternative to full model fine-tuning.

As its name says, however, the goal of transfer learning is to handle tasks that are not the ones for which the model was pre-trained, or to modify the behavior of the model, whereas the **main goal of AfterLearnER is to improve the outputs of the model on the very same task for which it was initially trained, possibly using a non-differentiable \mathfrak{N} -loss that better describes its desired behavior.** Also, the \mathfrak{N} -parameter that AfterLearnER tunes is generally much smaller than that of the above works, even when considering that most weights are frozen.

2.1.2 Test-Time Training / Adaptation. Whereas fine-tuning and transfer learning pertain to supervised learning in that they require labeled examples of the new task, there are many real-world situations where such labels are not available. A large body of work has been devoted to such contexts, in particular, to handle the case of distribution shift between training and testing times, pertaining to *unsupervised domain adaptation*. A survey and discussion of several of such approaches is given in [Niu et al. 2022].

A first line of research assigns some labels to the unlabeled test data and performs some *test time training*. Such labels can be self-supervision labels, e.g., the number of 90° rotations in images [Sun et al. 2020] and the upper layers of the pre-trained model are gradually modified by standard backprop; or one can use some pseudo-labels obtained from a copy of the pre-trained model that is gradually updated [Chen et al. 2022]. However, in both cases, the size of the \mathfrak{N} -parameter is rather large (a large fraction of the original model), and the \mathfrak{N} -loss must be some usual supervised training loss, hence differentiable.

On the other hand, *test-time adaptation (TTA)*, as proposed by Wang et al. [2021], and further refined by, e.g., Niu et al. [2022, 2023], performs some generic entropy minimization, and only optimizes some affine transformation parameters of the normalization layers of the original deep network, in order to fully preserve the pre-trained model. The TTA \mathfrak{N} -parameter is hence very small, a feature shared with AfterLearnER. However, the entropy minimization is gradient-based,

and the \mathfrak{N} -loss is limited to the chosen entropy — or possibly another differentiable loss [Goyal et al. 2022].

The main advantage of AfterLearnER compared to test-time adaptation remains the possible use of non-differentiable \mathfrak{N} -loss, together with, in most cases, the small amount of data needed and the small compute needed (see Section 5).

2.1.3 Retrofitting in NLP. Retrofitting in Natural Language Processing enhances word vector representations by refining them with relational information from semantic lexicons. This post-hoc technique adjusts pre-trained word vectors so that semantically related words are closer in the representation vector space.

Faruqui et al. [2015b] introduced a graph-based retrofitting method that refines the word vectors using belief propagation on a graph constructed from the lexical relationships, encouraging linked words to have similar vector representations. This process retains the original distributional properties while integrating relational information. ConceptNet [Speer et al. 2017], a multilingual knowledge graph, links words and sentences through labeled edges and improves the understanding of word meanings. Combined retrofitting with word embeddings forms a hybrid semantic space called ConceptNet Numberbatch, which provides a richer understanding of language.

In summary, retrofitting for NLP leverages external knowledge to refine word representations, enhancing their quality and interpretability for various NLP tasks. Both AfterLearnER and the above works aim to take new knowledge into account to improve the task the model was pre-trained on by modifying a few of its parameters (the \mathfrak{N} -parameters). However, AfterLearnER can modify any type of \mathfrak{N} -parameter and is not limited to modifying the latent representation of the model. Furthermore, AfterLearnER uses far less new knowledge than the full lexicons required by NLP retrofitting approaches [Chiu et al. 2019].

2.2 Non-differentiable loss functions

Stochastic gradient descent and its many variants perform extremely well for many machine learning tasks, but can only handle differentiable loss functions. Non-differentiable criteria used in depth estimation (Section 5.1), simulators as in first-person shooters (Section 5.3), or criteria based on compilers as in code translation (Section 5.4), or human satisfaction as in image generation (Sections 6.1 to 6.3) are beyond gradient-based approaches.

2.2.1 Reinforcement Learning from Human Feedback. A particular case of non-differentiable loss function is the one built from human feedback. Reinforcement learning from human feedback (RLHF) has recently gained importance in image generation [Lee et al. 2023b] and large language models (LLMs). However, most low-budget RLHF papers (working with dozens or hundreds of human feedback samples) are in the field of robotics [Jain et al. 2015]. The trend in LLMs is more in the dozens of thousands, or even the millions [Abramson et al. 2022], though limited human feedback is sometimes sufficient [Kim et al. 2023] and real-time user-specific preferences can sometimes be taken into account [Videau et al. 2023]. Low-budget RLHF can be based on inverse reinforcement learning (IRL) i.e., simulating human preferences from preference signals in a reward model [Adams et al. 2022]. To reduce the need for abundant ground truth data, it is important to focus on small but impactful weights of the model as \mathfrak{N} -parameter. As already mentioned in Section 2.1.1, Burkholz [2024]; Giannou et al. [2023]; Lu et al. [2022] present such possible small impactful parts, for instance, the normalization layers, which intersect entirely the information flow from input to output.

2.2.2 Indirectly using gradients. On the other hand, several workarounds have been proposed to handle non-differentiable losses. The principle of reward shaping, in various contexts such

as non-differentiability or delayed reward, is to modify the loss function, to make it easier to optimize. Using approximations or modifications of the real loss is, however, risky, as pointed out by [Skalse et al. 2023]: the solution to the reformulated problem might not be a solution for the original problem. In terms of optimization algorithms, Rolinek et al. [2020] propose a method specific to rank-based criteria. Jiang et al. [2020] and Huang et al. [2021] propose to approximate non-differentiable loss functions by differentiable ones. Hiranandani et al. [2021] focuses on criteria defined on the confusion matrix. Sun et al. [2022] focus on a random subspace of a huge parameter space. Susano Pinto et al. [2023] apply the Reinforce [Williams 1992] algorithm. Also, in [Lee et al. 2023a; Niu et al. 2023; Wang et al. 2021], differentiable criteria are designed as proxies to the actual target loss functions, adding one level of approximation to the goal, and hence possibly leading to less accurate solutions. On the other hand, AfterLearnER explicitly handles the non-differentiable \mathfrak{N} -loss, based on generic black-box optimization (Section 2.3).

2.2.3 Hyperparameter Tuning. Hyperparameter optimization (HPO) has become routine in the ML world in general (see e.g., Feurer and Hutter [2019] for a survey), and in deep learning in particular. The \mathfrak{N} -parameter, in such context, is made of the usual hyperparameters of the training pipeline and can include architecture parameters (HPO is then called neural architecture search (NAS)). The optimization is then a two-tiered process, as shown in Figure 1-top, in which the inner loop is a full backprop optimization, and the outer loop is a black-box optimization (e.g., Bayesian [Kandasamy et al. 2018] or Evolutionary [Assunção et al. 2019]). But the process is extremely costly because the \mathfrak{N} -loss is then the performance of the fully re-trained network. As such, we do not consider it as an alternative to AfterLearnER, nor do we compare AfterLearnER with HPO approaches as they do not tackle the same problems.

2.3 Tools for black-box optimization

Black-box optimization (BBO) refers to optimization methods that only need, from the loss function f (aka the objective function in the optimization world), the value of $f(x)$ for any given x . In particular, no gradient is used, and no knowledge of the internal structure of f is necessary. Many approaches have been proposed in the literature, from Mathematical Programming (deterministic methods that offer guarantees but sometimes poorly scale up (unless the problem to solve has some good mathematical properties) to Metaheuristics (i.e., stochastic approaches that often experimentally outperform Mathematical Programming methods but hardly find the exact solution), and many intermediate algorithms. Among the most popular metaheuristics are Evolutionary Algorithms [Bäck et al. 1997; Eiben and Smith 2015; Goldberg 1989; Schwefel 1995], and Iterated Local Search [Stützle and Ruiz 2018], including Simulated Annealing [Kirkpatrick et al. 1983], Tabu Search [Glover and Laguna 1997], Differential Evolution (DE) [Storn and Price 1997], and Particle Swarm Optimization (PSO) [Kennedy and Eberhart 1995].

Algorithm 5 in Appendix B outlines the functioning of the optimization algorithms used in this study, within a parallel computing context, using the well-known *ask-and-tell* interface: the algorithm o is defined by its methods *initialize*, *tell* (informs o of the value of $f(x)$), *ask* (returns next value x to evaluate), and *recommend* (returns its best guess for the optimum). There are many libraries for black-box optimization. AfterLearnER uses Nevergrad [Rapin and Teytaud 2018] that implements, among others, Evolutionary Algorithms [Eiben and Smith 2015], Mathematical Programming [Powell 1964, 1994], and handcrafted combinations [Meunier et al. 2022b].

In terms of black-box optimization tools, AfterLearnER can perform several internal runs using different optimizers, as developed in Algorithm 1. By default, it uses a single algorithm, namely the optimization wizard (Appendix C) NGOpt [Meunier et al. 2022a], which automatically selects a relevant algorithm based on the available computational budget, the problem dimension, and the

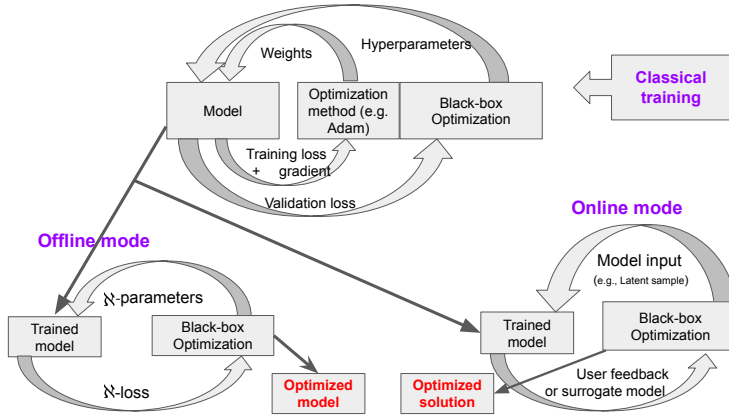


Fig. 1. AfterLearnER vs. Classical ML. **Top:** Standard gradient-based training (e.g., backpropagation) and hyperparameter tuning (the outer loop). **Bottom:** The two modes of AfterLearnER. **Left:** In the *offline mode*, retrofitting of some parameters (termed \mathfrak{N} -parameter, see text) of the trained model, once and for all before test time, as in Sections 5.1 to 5.4, and the output of AfterLearnER is an optimized model. **Right:** In the *online mode*, the \mathfrak{N} -parameter can also include some model input in the latent space, the objective can then be dynamic (the loss, the user feedback, or a surrogate model), as in Sections 6.1 to 6.4. The output of AfterLearnER is then an improved output for the given input.

types of variables to optimize. Other algorithms are used in some cases, for the sake of comparison: (1+1) refers to the (1+1)-evolution strategy with one-fifth rule [Rechenberg 1973], Discrete(1+1) is a classical evolutionary algorithm with mutation rate $1/d$ in dimension d (see discussions in [Doerr et al. 2019; Einarsson et al. 2019]), DiagonalCMA (the diagonal version of Covariance Matrix Adaptation Evolution Strategies) [Hansen and Ostermeier 2003; Ros and Hansen 2008], Differential Evolution (DE) [Storn and Price 1997], Particle Swarm Optimization (PSO) [Kennedy and Eberhart 1995], Lengler which extends the Discrete(1+1) to a decreasing mutation rate [Einarsson et al. 2019]; TBPSA refers to Test-Based Population Size Adaptation as in [Khalidov et al. 2019], Powell [Powell 1964], SQP (Sequential Quadratic Programming [Artelys 2015a]), GeneticDE which combines several variants of DE, Coby [Powell 1994]. They are chosen according to the recommendations described in the Nevergrad documentation, as detailed later (Section 5.3.4 or Section 5.4). We sometimes use the baseline Zero for validation: this is a naive method just recommending the center of the search space, we should, therefore, always do better than this. Some algorithms used in our experiments also use prefixes as follows. “Optim” means “Optimistic” [Munos 2014], Disc. refers to Discrete [Rapin and Teytaud 2018], “Recomb” refers to recombinations by crossover [Holland 1975]. “Port” refers to Portfolio, which is the name used in Nevergrad for the choice of mutation rate in [Dang and Lehre 2016], “Split” refers to an automatic decomposition in blocks of variables [Rapin and Teytaud 2018], “Prog” refers to progressive optimization inspired by [Wang et al. 2009], “Noisy” refers to a combination with bandit algorithms related to [Cauwet and Teytaud 2016; Chiu et al. 2015; Heidrich-Meisner and Igel 2009]. We use $k < 50$ runs (see k in the table) and pick up the one with the best validation \mathfrak{N} -loss, as in Algorithm 1. The names of all methods are those in Nevergrad [Rapin and Teytaud 2018].

3 THE AFTERLEARNER ALGORITHM

3.1 Overview

The overall view of AfterLearnER is given in Figure 1. AfterLearnER can operate before test/inference time (bottom left) or at test/inference time (bottom right) – more details below. In both cases, the user should proceed as follows:

- Select the \mathfrak{N} -parameter, a small subset of the hyperparameters and/or model parameters to be fine-tuned. Several examples of such \mathfrak{N} -parameter are given in the experimental Sections 5 and 6 and detailed in Table 2.
- Choose a focused, reliable, possibly non-differentiable \mathfrak{N} -loss function (e.g., from human feedback) as the objective of the retrofitting. In particular, it can (and is) be different from the loss used for training the model, which is required to be differentiable.
- Find approximately the optimal values of the \mathfrak{N} -parameter using a black-box optimization algorithm to minimize the \mathfrak{N} -loss, using only the results of a few inferences on a validation set, in particular without ever retraining the whole model.

AfterLearnER always operates on the fully trained model, i.e., **after the classical backprop training**. As said, there are two modes in AfterLearnER. In *offline mode* (Figure 1-bottom left, examples in Sections 3 and 5.1 to 5.4), AfterLearnER optimizes the \mathfrak{N} -parameter w.r.t. the \mathfrak{N} -loss once and for all, using some low-volume coarse-grain validation data. In particular, it only needs a few inferences of the trained model (and in particular, no gradient backpropagation).

In the *online mode* (Figure 1-bottom right and Sections 6.1 to 6.4), AfterLearnER optimizes the model answer to each test example during inference, and the \mathfrak{N} -parameter can typically contain some latent variables, input to the model. This amounts to online retraining based on some small aggregated feedback (see Section 3.3.4).

Note that these two modes are not very different. In both cases, for optimal performance on an application, we optimize it using the actual satisfaction criterion. When there is one actionable user feedback (e.g., for image generation, see the experiments in Section 6), it is used to construct the \mathfrak{N} -loss: this is the **online mode**. On the other hand, when playing Doom (Section 5.3) or estimating depth (Section 5.1), getting user feedback on a significant part of the results would take a significant time. AfterLearnER is then run in **offline mode**, based on data previously gathered. The main difference is that the \mathfrak{N} -loss, and hence the criterion for success (see also Section 4.2.3), can be computed in the offline mode, whereas it will be based on human ratings, and hence, rather slowly, in the online mode. In both cases, the implementation follows Algorithm 1 detailed below, which is, codewise, implemented in a few lines as shown in Section 2.3; for a deep learning model stored in GPU memory, we need two more lines for reading/writing directly the weights as shown in Appendix G.

3.2 The Algorithm

The AfterLearnER algorithm and its default hyperparameter settings are presented in Algorithm 1. Given an \mathfrak{N} -loss to be minimized on some validation set \mathcal{V} (running the trained model at hand on the data points in \mathcal{V}), AfterLearnER needs an integer k (the number of times the embedded optimizer(s) will be launched within one run of AfterLearnER, hereafter called number of **internal runs**), a non-empty list of black-box optimization algorithms, and a list of possible budgets. It then loops k independent times (Line 1), launching (Line 4) one randomly chosen black-box algorithm in the list (Line 2) to minimize the \mathfrak{N} -loss on \mathcal{V} , until exhausting one of the available budgets (Line 3). The result of the run is stored (Line 5), and the best result of the k internal runs is returned by AfterLearnER (Line 7).

By default, the list of black-box algorithms is made of a single algorithm; the wizard *NGOpt* [Meunier et al. 2022a], presented in more detail in Appendix C. As a wizard, it can work in all dimensions/domains/budgets. The budget and the number of runs depend on the expected computational cost and the available overall compute budget. See Table 3 for some examples of AfterLearnER settings used in the present work.

Algorithm 1 The AfterLearnER algorithm.

Require: \aleph -loss ℓ
Require: \mathcal{V} validation set
Require: List of black-box optimization algorithms O ▷ By default $O = \{NGOpt\}$
Require: List of budgets B ▷ No default value
Require: Number of independent internal runs k ▷ By default 1

- 1: **for** $i \in \{1, \dots, k\}$ **do**
- 2: Randomly draw $o_i \in O$ ▷ only if $\#O > 1$
- 3: Randomly draw $b_i \in B$
- 4: Run o_i to minimize ℓ on \mathcal{V} with budget b_i
- 5: \aleph -parameter $p_i = o_i.recommend()$ ▷ The result of internal run i
- 6: **end for**
- 7: **return** \aleph -parameter $p = ArgMin_{i \in [1, k]} \ell(p_i)$ ▷ Best result in k internal runs

3.3 Rationale for AfterLearnER

The main advantage of AfterLearnER is that it works on the real end-user objective function, without requiring an adaptation to gradient-based optimization. This section discusses the other potential benefits of using retrofitting beyond the obvious generic advantages of any gradient-free optimization: in settings in which the gradient cannot be computed or does not make any sense; e.g., discrete metrics or discrete domains.

3.3.1 Computational cost. Even when the gradient exists and is easy to compute, it might require a large computational cost, and re-optimizing billions of weights for each value of the hyperparameters is time-consuming. AfterLearnER has a low computational cost: no gradient must be computed during AfterLearnER, therefore saving the memory and computation costs of the backward pass. Examples of budget are given in Table 3.

3.3.2 Theoretical Analysis of Overfitting Risk. Whereas gradient-based optimization does not lead to any bound on the generalization error, such bounds can be obtained when using black-box optimization, as detailed now. These bounds suggest that the risk of overfitting of AfterLearnER is low.

Indeed, consider δ_ϵ the risk of an ϵ -divergence between the empirical risk and the risk in generalization for a given \aleph -parameter:

$$\delta_\epsilon = P(|(\text{expected loss}) - (\text{empirical loss on dataset})| > \epsilon)$$

If we use the validation error for picking up the best \aleph -parameter, in a list of N \aleph -parameters (eg this list is created by random sampling as in random search, or by low-discrepancy search), the risk of deviation ϵ for that \aleph -parameter is at most $N \cdot \delta_\epsilon$ (Bonferroni correction [Bonferroni 1936]) instead of δ_ϵ :

$$P(\exists \aleph\text{-parameter } c, |(\text{expected loss})_c - (\text{empirical loss on dataset})_c| > \epsilon) \leq N\delta_\epsilon$$

If the N \aleph -parameters are not defined a priori but built by optimization, with λ \aleph -parameters per iteration and selection of the best at each iteration, then, assuming the optimization algorithm is deterministic, the number of possible internal states of the optimization algorithm after the choice of one \aleph -parameter among λ possible choices is λ . Hence the list of M possible internal states after n iterations has length λ^n [Fournier and Teytaud 2011]. The total risk is therefore at most $\lambda^n \cdot \delta_\epsilon$ where n is the number of iterations.

This proof is valid for deterministic optimization algorithms, with internal states and final output depending only on the selection of one \aleph -parameter at each of the n iterations. In the deterministic case, the random part only depends on the evaluation of a dataset, which is possibly randomized, and on the sampling process providing the dataset. δ_ϵ refers to a probability for this probability universe. For a randomized optimization algorithm, the risk $\delta_{\epsilon,\omega}$ of a deviation ϵ also depends on ω , the random seed of the optimization algorithm. Then, we get an overall risk

$$\delta_\epsilon = \mathbb{E}_\omega \delta_{\epsilon,\omega}. \quad (1)$$

However, the deterministic reasoning above also holds for a stochastic optimization algorithm for any fixed random seed ω , and therefore Equation (1) makes it also valid for a stochastic optimization algorithm.

And if the total number N of evaluations is fixed at N , then $n = N/\lambda$ and the total risk is at most $\lambda^{N/\lambda} \cdot \delta_\epsilon$.

Furthermore, if AfterLearnER performs $k > 1$ independent optimization runs (see internal runs in Algorithm 1), and if the budget B is divided by k , then the Bonferroni correction leads to a risk bounded by

$$\underbrace{k}_{\text{Bonferroni correction for } k \text{ runs}} \cdot \underbrace{\lambda^{(B/(\lambda \cdot k))}}_{\text{Branching factor per run}} \cdot \underbrace{\delta}_{\text{Risk for a single model}} \quad (2)$$

for the resulting parametrization. These equations, interestingly, lead to upper bounds less than 1 in many cases of interest (e.g., Hoeffding bound for upper bounding δ_ϵ , and a dataset size 8000, and $\epsilon = 0.05$, and $\lambda = 2$ and budget $B = 100$, lead to a bound < 0.01 .) According to these bounds, increasing the number k of independent runs for a fixed total budget decreases the risk of overfitting. This is particularly visible in Table 4, for the Speech Resynthesis problem, for which overfitting is critical. Also, according to this bound, increasing the parallelism λ decreases the risk of overfitting. A drawback, however, is that increasing the number of runs makes the results closer to a random search and, therefore, possibly less precise.

3.3.3 Versatility, convenience. Black-box optimization is a very versatile approach, allowing the user to easily explore different objective functions. For Doom (Section 5.3), for fair comparisons, we report results on the same losses as the ones used by the authors of previous works [Lample and Chaplot 2017]. However, a significant benefit of AfterLearnER is its ability to adapt a model to a different loss, the \aleph -loss, without the need to manually craft reward shaping or to use an approximate proxy.

We note that the approach can be applied for the optimization of a complex system, including several deep learning models combined with other mathematical programming tools or signal processing methods, even if some of these blocks are non-differentiable, as illustrated by the experiments presented in Section 5.

3.3.4 Small Aggregated Anytime Feedback. In summary, the potential benefit of AfterLearnER is that it only needs feedback with the following properties:

- **Small:** A few dozen scalars is enough, as will be demonstrated in the experiments (see Table 2).

- **Aggregated:** A feedback of one scalar per model is sufficient, instead of one scalar per data point or one scalar and a gradient for each mini-batch. This is visible in our applications when training once and for all a model between training and testing, in Sections 5.1 to 5.4 and 6.1.
- **Anytime:** AfterLearner can be stopped when desired, given the real-time user feedback [Zilberstein 1996].

The purpose of the rest of the paper is to validate experimentally AfterLearnER on eight diverse use cases that highlight these properties.

4 EXPERIMENTAL SETTINGS

AfterLearnER will now be validated on eight use cases whose main characteristics (including the \mathfrak{N} -parameters) are given in Table 2, while the corresponding AfterLearnER hyperparameters used in their respective experiments are given in Table 3.

4.1 AfterLearnER User Guide

The choice of these test beds and their setups has been guided by the following principles, which can be viewed as a kind of User Guide for AfterLearnER.

- (1) **Optimize a small but impactful part:** Burkholz [2024]; Giannou et al. [2023]; Lu et al. [2022] have demonstrated how a small part of the parameters of an ML model (i.e., a small number of weights) can have a big impact on its performance. Typically, for a huge network or a combination of modules, one should look for the smallest set of weights that intersect all paths from inputs to outputs. Furthermore, it is important to keep the dimension of the optimization problem small: black-box optimization algorithms do not scale up very well in general — opposite to gradient-based optimization algorithms. The second column of Table 2 describes the \mathfrak{N} -parameters of all use cases, while the third column shows that, except for Doom, the volume of feedbacks is small compared to e.g., Arakawa et al. [2018]; Zhu et al. [2023].
- (2) **Don't fear non-differentiable \mathfrak{N} -losses:** This is the main advantage of AfterLearnER: Burkholz [2024]; Giannou et al. [2023]; Lu et al. [2022] optimize a small set of parameters (as we do), but with differentiable criteria. There are many methods for differentiable optimization in machine learning, and gradient-free algorithms cannot outperform these methods unless the gradient is unreliable. We note that Lee et al. [2023a]; Niu et al. [2022, 2023] propose to create (possibly without any human feedback or ground truth, thanks to unsupervised entropy minimization) a differentiable criterion based on entropy. However, AfterLearnER focuses on cases in which a non-differentiable criterion is worth a direct optimization.

4.2 Experimental Protocol

4.2.1 Baselines. Because AfterLearnER starts from a fully trained model, this model is the baseline to which AfterLearner should be compared. We have used, as far as possible, the implementations that the authors have provided on the internet (e.g., on GitHub). Each run is detailed in turn in the corresponding sections.

4.2.2 Comparison Metrics. There are two fundamental metrics that can be used to compare AfterLearnER with the baselines: (a) the **training loss** that was used to train the model that AfterLearnER tries to improve, and (b) the **\mathfrak{N} -loss** used by AfterLearnER during its optimization process. One may point out that both metrics are challenging to compare. First, AfterLearnER could not rapidly obtain positive results without benefiting from the excellent initial point provided by the baseline. Second, standard training and AfterLearnER do not have the same objectives: the \mathfrak{N} -loss is supposedly

Table 2. The size of the \mathfrak{N} -parameters optimized by AfterLearnER varies between 1 and 16384. All the feedbacks in this table are not differentiable. For comparison, a classical ML training with e epochs on a dataset of cardinal S and a gradient of size p has a feedback of size $(\mathbb{R} \cdot \mathbb{R}^p)^{e \cdot S}$.

Problem	\mathfrak{N} -parameter	Feedback volume	Type of feedback
Depth sensing	6 input normalization parameters	300 feedbacks by the large model (\mathbb{R}^{300})	Depth estimate by the large model
Speech resynthesis	2 real values (formerly hard-coded)	40 automatically computed feedbacks for TextLess	Word Error Rate
Doom AI	Rescaling of the output layer (35 weights)	Kills per life in VizDoom, in \mathbb{R}^{60000}	VizDoom simulation
Code Translation	Rescaling between encoder & decoder (1024 weights)	BLEU + comp. accuracy on valid set, in \mathbb{R}^{1000}	Automatically computed score
Facial Composites (offline fairness, Algorithm 3)	Single random seed	5 user clicks among 30 screens	Human preference for the initialization
EG3D-cats, global modifs	Latent variable z (problem dependent)	Image quality: 200 user inputs, one per image	Surrogate model
EG3D-cats, local modifs	Latent variable z (problem dependent)	Image quality: 200 user inputs, one per image	Surrogate model
Latent Diffusion Model, 200 images	Latent variable in $\mathbb{R}^{4 \cdot 64 \cdot 64}$	z , Image quality: 200 user inputs, one per image	Human rating + surrogate
Latent Diffusion Model, 15 images	Latent variable in $\mathbb{R}^{4 \cdot 64 \cdot 64}$	z , Variable, a few clicks	Human rating

Table 3. Typical AfterLearnER parametrization for the test cases of Section 5 and Section 6 (as several runs are considered, the budgets are not all the same). The specific case of LDM-15 uses an additional ‘‘Voronoi crossover’’ described in Section 6.4.

* 10000 for EG3D is an upper bound: The actual number is frequently just a few dozen.

** for this application to LDM, 200 is the number of human feedbacks used in the offline mode for training the surrogate model, which is then used online at each generation.

Problem	List of Optimizers O	List of Budgets B
Depth sensing	$\{NGOpt\}$	$\{50\}$
Speech resynthesis	$\{NGOpt\}$	$\{2, 10, 20, 40, 80\}$
Doom AI	$\{OptimDisc(1 + 1)\}$	$\{300, 600, 800, 1000, 1200\}$
Code translation	$\{DiagonalCMA\}$	$\{1000\}$
Facial Composites Fairness	$\{RandomSearch\}$	$\{30\}$
EG3D-cats, global modifs	$\{RandomSearch\}$	10000*
EG3D-cats, local modifs	$\{NGOpt\}$	10000*
Latent Diffusion Models - 200	Lengler (surrogate model)	200 images**
Latent Diffusion Models - 15	Lengler (with crossover)	a few batches (≈ 15 images)

closer to the actual goal of the user than the training loss, which is either a differentiable proxy for the \mathfrak{N} -loss (in the offline mode), or lacks user input (in the online mode). However, because user satisfaction is our ultimate goal, we will use the latter and compare AfterLearnER with the corresponding baseline using the \mathfrak{N} -loss.

4.2.3 Comparing \mathfrak{N} -losses. For each use case, the performances of the model optimized by AfterLearnER (in terms of \mathfrak{N} -loss, as argued above) are evaluated against the baselines on several different scenarios, or *contexts* that will be described in the respective sections. These contexts

can involve different hyperparameters of AfterLearnER (such as the number of internal runs k , the different budgets for the different internal runs B , or the possible choices of the embedded optimizer O , see Algorithm 1), or different situations depending on the problem at hand. For each context, a small number of independent runs of AfterLearnER are performed on a validation set, and the average \aleph -loss (with std. dev.) on a separate test set are reported, as one can see below.

4.2.4 P-values. As stated in Algorithm 1, one run of AfterLearnER launches k internal runs with budgets b_1, \dots, b_k , and thus its total budget is $N = \sum_{i=1}^k b_i$. Thus, despite the low cost of AfterLearnER compared to a full backpropagation training procedure, such repeated experiments are still costly, and in some (though not all) of our experimental contexts, a rather small number of independent runs of AfterLearner itself is performed, **making comparative statistically significant tests impossible for some unique contexts**. Nevertheless, when considering several contexts simultaneously, it becomes possible to test the statistical relevance of our findings by computing the p-values through a binomial test (Fisher’s exact test), with the null hypothesis being “the model improved by AfterLearnER does not outperform the baseline on a given context with probability $\geq \frac{1}{2}$ ”. We refer to this measure simply by “**p-value**” in the following, in the absence of any ambiguity.

4.3 Outline of experiments

Next two sections present the experimental validation of AfterLearnER on eight test cases. Section 5 details four experiments that pertain to the **offline mode**, and directly use Algorithm 1: Depth Sensing (Section 5.1), Speech Resynthesis (Section 5.2), Doom (Section 5.3), and Code Translation (Section 5.4).

Section 6 in turn describes the four experiments that the **online mode** of AfterLearnER, which is then tightly embedded in the inference process: Facial Composites (Section 6.1), 3D-GANs with EG3D (Section 6.2), Latent Diffusion Models (LDM) with a surrogate model learnt on human feedback (Section 6.3), and Interactive LDM (Section 6.4).

5 OFFLINE MODE EXPERIMENTS

5.1 Depth sensing

5.1.1 Context. MiDaS [Ranftl et al. 2022] is a famous deep network for monocular depth estimation from a single image. This neural network exists in three trained variants: large, hybrid, and small. The large one, known for its precision [Birkel et al. 2023], is considered here as the ground truth.

Following [Ranftl et al. 2022], ImageNet images are first resized to 144×144 pixels. Then, AfterLearnER (Algorithm 1) uses a set \mathcal{V} of 300 images randomly drawn from the ImageNet validation set (of size 50,000). With $b = 50$, the feedback used by AfterLearnER is made of the 50 scalars obtained in applying 50 variants of the model (corresponding to different \aleph -parameters iteratively provided by AfterLearnER) to the images in \mathcal{V} , for each of the k internal runs. Furthermore, a set \mathcal{V}' of 500 images randomly drawn from the ImageNet test set are used to assess AfterLearnER performance.

5.1.2 \aleph -parameter. AfterLearnER tunes the 6 normalization parameters (multiplication and bias for each of 3 channels) for optimizing the \aleph -loss on \mathcal{V} .

5.1.3 \aleph -loss: Estimating depth. Yin et al. [2020] point out that there exist several depth estimation criteria created for different applications: a criterion that is good for local differences (relative depth) might be plain wrong for global profiles. Therefore, a diversity of criteria has been proposed, including, among others, the absolute relative error (AbsRel), the weighted human disagreement

rate [Xian et al. 2018], the scale-invariant root-mean-square error [Li et al. 2019], or the frequency of obtaining a mismatch greater than a given threshold [Ranftl et al. 2022]. These different losses are used in different areas [Hwang et al. 2021; Ma and Karaman 2018; Paul et al. 2022].

Following [Ranftl et al. 2022], we focus here on the frequency of failing, by a factor greater than 1.25^i , with $i = 1, 2$, or 3 (further referred to as Threshold i). These criteria are not continuous and are flat almost everywhere, so that their gradient is essentially zero. The baselines corresponding to the different Thresholds are computed using the code available at github.com/isl-org/MiDaS.

5.1.4 Results. AfterLearnER (Algorithm 1) is launched here with values $O = \{NGOpt\}$, $B = \{b\}$ (by default 50), for different values of k .

Figure 2 displays the \mathfrak{N} -loss on the test set \mathcal{V} versus the number of internal runs k , each one with a budget of 50 (other results are presented in Appendix A). These results demonstrate an enhancement in the \mathfrak{N} -loss optimized using the validation set, consistently improving the performance of the Small baseline and sometimes outperforming the performance of the Hybrid model, even with $k < 10$. Appendix A also presents evidence of effective transferability: specifically, training on Threshold 3 (i.e., with ratio 1.25^3) not only improves the outcomes in the test set for that metric but also yields positive results for other metrics discussed in Section 5.1.3 above.

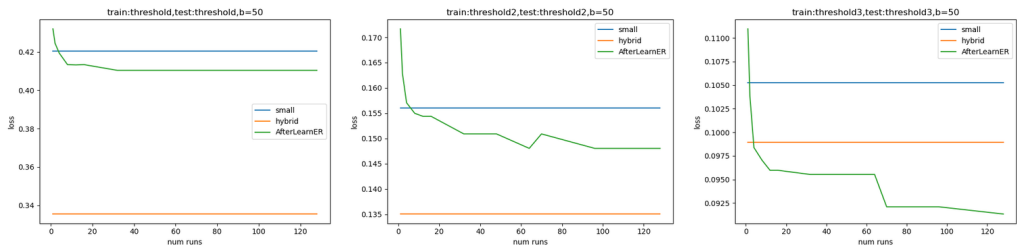


Fig. 2. Depth Sensing: Average (over 60 runs) \mathfrak{N} -losses on the test set \mathcal{V} of the **small** and **hybrid** models (the baselines), and of **the model optimized by AfterLearnER** on Thresholds 1 (left), 2 (middle) or 3 (right), for different values of k (x-axis), with $b = 50$.

5.1.5 Discussion. Whereas AfterLearnER needs no more than 50 scalars of feedback in order to improve the Small model, a larger budget allows it to sometimes outperform the Hybrid model with just 300 scalars (e.g., $k = 6$ and $b = 50$ in Figure 2). And though we used in the present case the large MiDaS model as a ground truth for the sake of reproducibility, if the feedback were to be asked to human raters, it would remain a reasonable effort for small k s.

Furthermore, we observe that results are robust and are effectively transferred to different loss functions (Appendix A).

5.2 Speech resynthesis: a few dozen of feedbacks for improving sound quality

TextLessLib [Kharitonov et al. 2022] is a deep learning library for speech synthesis without text representations. It includes a demo of speech resynthesis [Polyak et al. 2021] from low bit rates.

5.2.1 Context. The discrete resynthesis operation can be viewed as a form of lossy compression for speech. Approaches such as that of Polyak et al. [2021] directly train in the waveform using an autoencoder, with adversarial and reconstruction loss. Here, we directly optimize the Word Error Rate (WER) [Kharitonov et al. 2022], which is not differentiable. We use data and code from [Polyak et al. 2021], splitting the training data into 75% for the \mathfrak{N} -parameter optimization and 25% as a post-optimization test set. The results can, therefore, not be compared numerically to the results in

the original work as we use additional information. Nonetheless, the results show that a few dozen scalar feedbacks are enough for a significant improvement.

5.2.2 \aleph -parameter. AfterLearnER handles here two parameters of the Tacotron/Vocoder model [Wang et al. 2017]: the sigma in WaveGlow/inference [Prenger et al. 2019] and the denoiser strength. These two parameters are hard-coded in the original code.

5.2.3 \aleph -loss: Word-Error-Rate. This measure evaluates how accurately the audio can be transcribed after compression, assessing how well the textless compression preserves speech-specific characteristics and clarity. WER is computed through the wav2vec 2.0-based [Baevski et al. 2020] and Automatic Speech Recognition (ASR) system: the code compares the output with the ground-truth transcription. The WER is also used to evaluate the retrofitted model on the test set.

5.2.4 Results: robust low budget quality improvement. The results of different parameterizations of AfterLearnER are presented in Table 4. One can observe that picking up the best outcome from multiple shorter internal runs (i.e., a large k with a small budget b per run) yields the most favorable results. In certain instances, the internal number of runs k is even so large, and the budget per run so limited that the approach resembles a random search (e.g., a 9.9% improvement observed with the best of 8 runs each having a budget of 2). These experiments demonstrate that AfterLearnER can significantly improve test results at a low \aleph -loss within a few evaluations on a small validation set.

5.2.5 Discussion. Table 4 shows that for this use case with minimal sample size, the utilization of a high number of runs (and a smaller b) consistently enhances performance in generalization, aligned with the theoretical discussions presented in Section 3.3.2: such results experimentally demonstrate the reduction of the risk of overfitting by using a large number of runs and a small budget per run.

5.3 Doom AI: Retrofitting for Deep Reinforcement Learning

5.3.1 Context. We explore the application of AfterLearnER in the context of the game “Doom”, in the framework defined by Lample and Chaplot [2017]. Our study focuses on two distinct setups: “Normal mode”, where the agent combats 10 bots, and “Terminator mode”, involving a confrontation with 20 bots. As the base trained network, we use the agent defined in [Lample and Chaplot 2017], which is trained in *Normal mode*.

5.3.2 \aleph -parameter. We add a flattened action head of length 35 in the final layer of the baseline network, where the output o (of dimension 35) is adjusted to $o \cdot \exp(r)$: These 35 scalars are the \aleph -parameter to optimize.

5.3.3 \aleph -loss: Kill/Death ratio. Since the main objective in Doom is to kill as many bots as possible while minimizing your own deaths, we optimize the non-differentiable and long-term objective of the kill/death ratio. However, this reinforcement signal is very noisy: when $k > 1$, it might happen that the comparison between the different signals on the last iteration of each internal run, is a wrong indicator of which of the k runs is the best one. So, instead of the last value of this kill/death ratio, we use a moving average of the last 8 values as the \aleph -loss returned to the black-box optimizer.

5.3.4 Results: AfterlearnER kills monsters in Doom. A clear improvement can be seen in Table 5. In that Table, the suffix 10 (resp. 100) refers to dividing the scale by 10, i.e., we use $\exp(0.1r)$ (resp. $\exp(0.01r)$) instead of $\exp(r)$. The suffix w20 means that we use $P = 20$ parallel workers inside each of the k internal runs, as opposed to a single worker: this reduces the wall-clock computational cost, but also the number of available feedbacks, as shown in Algorithm 5 in Appendix B. Note that these experiments are run in preemptable mode on the cluster, allowing for interruptions,

Table 4. Word Error Rate (N-loss) on the test set in textless Speech Resynthesis for different numbers of internal runs k and different budgets b per internal run. The baseline WER is 7.84. For each pair (k, b) , several independent runs are run (at least 6 per row – std dev in the last column): 100% of contexts lead to an improvement on average. The p-value (Section 4.2.4) over the 16 independent contexts, under the null assumption that the probability of improvement is not greater than .5, is significant ($p\text{-val} \leq 1.6e - 5$). Consistently with Section 3.3.2, we observe low overfitting and excellent performance for k large.

Internal runs k	Budget b	WER (↓)	Average improv. (% , ↑)	Std. dev. WER
3	2	7.488	4.511	0.335
	10	7.558	3.620	0.202
	40	7.736	1.361	0.235
	80	7.542	3.828	0.298
4	2	7.306	6.837	0.387
	10	7.501	4.355	0.147
	40	7.751	1.163	0.217
	80	7.378	5.924	0.201
5	2	7.222	7.908	0.397
	10	7.442	5.104	0.130
	40	7.803	0.502	0.149
6	2	7.273	7.259	0.417
	10	7.433	5.216	0.104
7	2	7.097	9.506	0.361
	10	7.398	5.661	0.076
8	2	7.067	9.880	0.344

hence the uncontrolled number of internal runs k in Table 5 (last column). We observe, nonetheless, positive results in almost all cases.

Here, we use a single black-box optimization method o in O for each experiment, but we repeat the experiment with distinct o for the sake of comparisons. We refer to Section 2.3 for more details about the different algorithms mentioned in Table 5.

5.3.5 Discussion. The terminator mode is a priori easier to optimize: the baseline agent was originally optimized for normal mode, a priori leaving a more significant gap of potential improvement by AfterLearnER for this transfer learning.

In terminator mode, the best results are obtained by methods based on DiscreteOnePlusOne. Therefore, we only used this optimization algorithm for the normal mode, and we can observe an improvement over the baseline in all cases. The validation score for TBPSA is the lowest: this is because TBPSA [Khalidov et al. 2019] explores widely and tries to learn from samples far away from the current optimum (as recommended in [Beyer 1998]). Its performance in the test is nonetheless among the top 4.

5.4 Code translation

5.4.1 Context. Transcompilers perform code translation, i.e., convert source code from one programming language to another while maintaining the same level of abstraction. Unlike traditional compilers, which translate high-level code to low-level languages like assembly, transcompilers focus on translating between languages of similar complexity. This process is useful for updating obsolete codebases or integrating code written in different languages. Roziere et al. [2020] leverage unsupervised machine translation techniques to develop a neural transcompiler. Trained on source

Table 5. Results on Doom. The red marker indicates the only detrimental run of AfterLearnER, which reduced test performance. For each of the 16 lines, we run AfterLearnER several times (at least 3 runs per row). The p-value over these 16 lines (Section 4.2.4) is less than 3.10^{-4} .

	Optimizer	Total budget $\sum_{i \leq k} b_i$	Validation score (\uparrow)	Average test score (\uparrow)	Number of internal runs k
	Baseline			3.61	
	DiagonalCMAw20	9348	2.447	3.642	11
	NoisyDisc(1+1)w20	6864	3.590	3.616	15
	Noisy(1+1)w20	10880	3.319	3.589	17
Terminator mode	OptimDisc(1+1)10	4500	3.700	3.719	11
	OptimDisc(1+1)w20	5980	3.712	3.682	13
	OptimNoisy(1+1)w20	6764	3.651	3.685	14
	ProgNoisyw20	8028	3.114	3.615	18
	RecombPortOptimNoisyDisc(1+1)10	5400	3.686	3.658	15
	RecombPortOptimNoisyDisc(1+1)w20	5696	3.630	3.639	17
	SplitNoisyw20	13144	3.234	3.646	18
	TBPSAw20	5964	2.404	3.678	15
	Baseline			3.31	
Normal mode	OptimDisc(1+1)100	51500	3.382	3.356	87
	OptimDisc(1+1)10	31200	3.419	3.399	50
	OptimDisc(1+1)w20	6644	3.380	3.430	20
	RecombPortOptimNoisyDisc(1+1)100	46900	3.453	3.447	75
	RecombPortOptimNoisyDisc(1+1)10	19950	3.346	3.329	36

code from open-source GitHub projects, their transformer model can accurately translate functions between C++, Java, and Python. This method uses only monolingual source code, requires no specific language expertise, and can be generalized to other programming languages. The present section uses this neural transcompiler as a baseline, and applies AfterLearnER before test/inference time (Algorithm 1) to improve its performance.

5.4.2 **\aleph -parameter: linear rescaling.** A linear rescaling layer (1024 weights) is added between the encoder and the decoder, and these 1024 scalars are the \aleph -parameter to be optimized.

5.4.3 **\aleph -loss: a diversity of criteria.** Many criteria can be used for code translation: computational accuracy, which checks that both programs’ outputs are equal for the same input, code speed, code size, BLEU [Papineni et al. 2002], which checks the correctness and readability of the code by measuring the similarity of n-grams between generated code and reference code, adjusting for length. Recent papers [Jiao et al. 2023] pointed out that overfitting or other issues can arise, making the joint improvement of robust and diversified criteria relevant, in particular on smaller but curated data sets. In this work, we use either the **computational accuracy** (frequency of obtaining a code which satisfies the requirements) or the **BLEU** [Papineni et al. 2002]². None of these \aleph -losses is differentiable.

5.4.4 **Results: AfterLearnER can code.** Figure 3 compares the solutions obtained using AfterLearnER (with different black-box optimizers o) to the baseline solution using a feedback limited to b ground

²From the abstract of [Papineni et al. 2002]: BLEU is a method of automatic machine translation evaluation that is quick, inexpensive, and language-independent, that correlates highly with human evaluation, and that has little marginal cost per run.

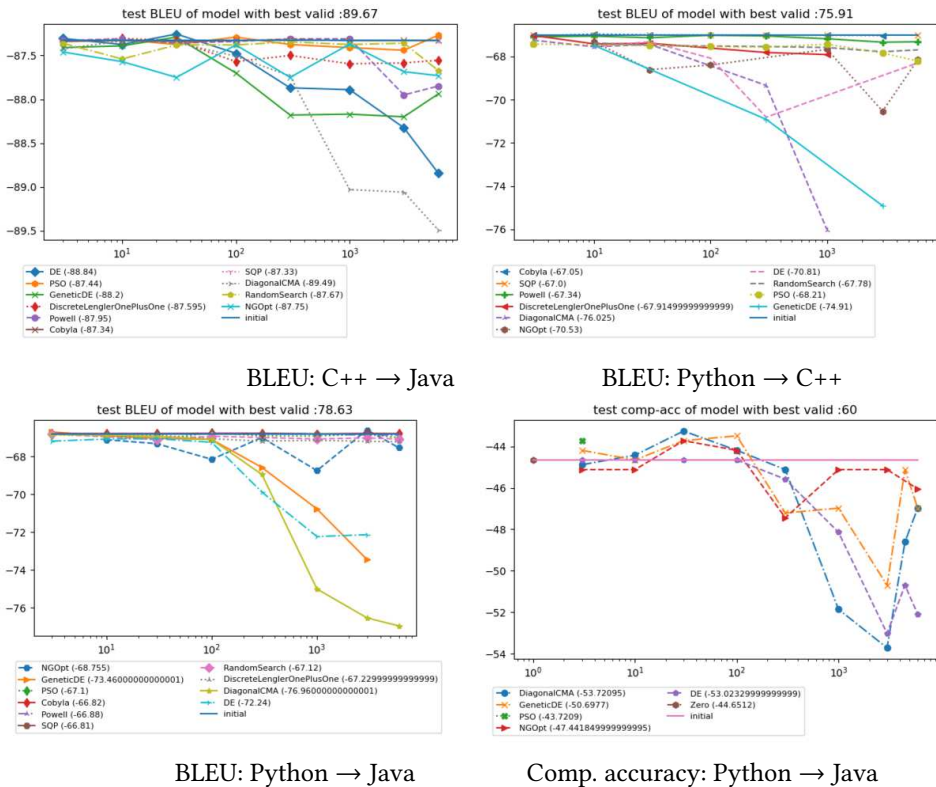


Fig. 3. Results of AfterLearnER on several problems from [Roziere et al. 2020] with BLEU or Accuracy \mathcal{N} -loss (the lower the better). Each curve is the average over 3 runs of AfterLearnER with $k = 1$ (i.e., one internal run) and the set O limited to a single optimization method. The horizontal line is the baseline, i.e., without any retrofitting. Note that if we remove Zero (which is a baseline run for validation, which does not modify the baseline) and SQP (which does not make sense for this dimensionality), AfterLearner is successful in 31 independent cases out of 32, with p -value $\leq 1e - 8$ (Section 4.2.4).

truth scalar numbers (b on the x -axis). O is restricted to a singleton $\{o\}$ (see o in the legend) and a single run ($k = 1$).

The results obtained with AfterLearnER improve over the baseline, whatever the optimizer used, though some optimizers perform better than others. Empirically, *DiagonalCMA* is often the best choice in this context.

5.4.5 Discussion. These experiments have been performed with the distribution of test cases in the original code from Roziere et al. [2020], i.e., code size limit at 100 tokens: we investigated the case of a limit 512, but further work is needed on the dataset as there are redundancies between validation and test in that context in particular when using computational accuracy, which aggregates distinct but functionally similar codes.

6 ONLINE MODE EXPERIMENTS

6.1 Evolutionary GAN: Facial Composites with Fairness

6.1.1 Context: Improving diversity in the latent space of Evolutionary Interactive GANs. Generative adversarial networks (GANs) [Berthelot et al. 2017; Karras et al. 2018; Mirza and Osindero 2014; Riviere 2019] are now a widely used generative model. Interactive GANs [Bontrager et al. 2018; Rozière et al. 2020] propose images to the user and repeatedly modify their proposals based on the user’s feedback. We first present such an interactive GAN, namely the one from [Rozière et al. 2020], presented in an instance of AfterLearnER in online mode, namely Algorithm 2.

Given that the human feedback is based on clicks, the black-box optimizer o must be a rank-based algorithm, i.e., it only uses comparisons between fitnesses, regardless of actual values. Likewise, the default value of o is Lengler’s method [Doerr et al. 2019] because it is the recommended variant of DiscreteOnePlusOne (see [Rapin and Teytaud 2018]). Despite the effectiveness of DiscreteOnePlusOne for taking into account user feedback on the fly, unfairness due to the lack of diversity remains an issue due to the so-called mode collapse. Thus, it is frequently challenging to get some image classes [Zameshina et al. 2022].

Therefore, we propose Algorithm 3, a variant of AfterLearnER for choosing the seed parameter s in Algorithm 2 so that it generates a more diverse initial population. Algorithm 2 can be seen as having a seed s as \aleph -parameter, that we optimize with a simplified AfterLearnER (Algorithm 3) as follows:

- As a proxy of Algorithm 2, we use the user feedback on the initial screen generated by Algorithm 2 for a specific random seed i .
- We optimize this random seed i by enumerating 30 possibilities and requesting user feedback: what are the 5 most diverse seeds?
- Then, the algorithm uses one of the 5 preferred seeds (randomly drawn).

The motivation for randomly using one of the 5 preferred seeds is to ensure that the code is still randomized and that repeated runs can have some diversity even in the first iteration. Note that later iterations are anyway randomized.

6.1.2 \aleph -parameter: The random seed. Before running Algorithm 2, we optimize the “random” seed that produces the most diverse initial images according to the user feedback, as described in Algorithm 3.

6.1.3 \aleph -loss: Interactive measure of diversity. To evaluate the efficiency of Algorithm 2, which now incorporates seed optimization from Algorithm 3, various facial categories were targeted, and the \aleph -loss measures the user’s satisfaction. We report the number of iterations over 25-image screens required to achieve satisfactory results in the user’s eye for each category. Here, we measure diversity considering up to four categories: Female Asian, Female Blonde, Male Black, and Male Blond (see Figure 11).

6.1.4 Results: fairness improvement on various categories. Preliminary runs show that it is frequently hard to reach, as far as we can tell from very long runs, some categories with the original version of the algorithm (Algorithm 2) when the initial population is not diverse enough. Hence our first experiment will check that several such categories can be reached with our optimized “random” seed obtained by Algorithm 3. On average, the algorithm achieves the desired outcomes within 3.0 ± 0.2 screen iterations over the four categories. We conclude that this limitation was primarily due to the initial set of faces on the presented screen belonging to the same category, thereby creating a high hurdle for diverging from that specific cluster.

Algorithm 2 Base algorithm from [Rozière et al. 2020] for generating images as desired by users. Users only click on their favorite image, on each screen.

Require: A black-box rank based optimizer o ▷ by default DiscreteLenglerOnePlusOne

Require: λ , number of images per screen

Require: $\mu < \lambda$ number of clicks (selected images) per screen

Require: a GAN converting latent variables $(c_i)_{1 \leq i \leq \lambda}$ to images

- 1: If s is not specified, $s \leftarrow \text{random}()$
 - 2: From s , generate first λ parametrizations c_1, \dots, c_λ
 - 3: **while** user not satisfied **do**
 - 4: Display $\text{GAN}(c_1), \dots, \text{GAN}(c_\lambda)$ to the user
 - 5: user clicks on μ images $(i_1, \dots, i_\mu) \in \{1, \dots, \lambda\}^\mu$
 - 6: Report to o that the fitnesses of $c_{i_1}, \dots, c_{i_\mu}$ are greater than those of c_j for $j \notin \{i_1, \dots, i_\mu\}$
 - 7: o gives back next λ parametrizations c_1, \dots, c_λ
 - 8: **end while**
-

Algorithm 3 AfterLearnER for seed optimization: after running this algorithm, the random seed (Line 1 of Algorithm 2) becomes “Initialize o with a random choice of s in an optimized subset of 5 seeds”.

Require: λ , number of images per screen.

Require: a GAN converting latent variables $(c_i)_{1 \leq i \leq \lambda}$ to images

- 1: Randomly choose s_1, \dots, s_{30} random seeds
 - 2: **for** $1 \leq i \leq 30$ **do** ▷ Surrogate of Algorithm 2 with random seed i
 - 3: GAN generates λ images using seed i ▷ similarly to Algorithm 2, Line 2.
 - 4: Display this screen to the user
 - 5: **end for**
 - 6: ask the user for the 5 most diverse screens i_1, \dots, i_5 ▷ Human Feedback
 - 7: Line 1 of Algorithm 2 becomes " $s \leftarrow \text{random-choice}([i_1, \dots, i_5])$ "
-

6.1.5 Discussion. This experiment is a combination of [Rozière et al. 2020] and a straightforward application of AfterLearnER to optimize its “random” seed: in spite of its simplicity, this approach solves a real diversity problem and is a reminder that taking care of a seed can have a big impact (as also reported in [Ventos et al. 2017], which applied seed optimization for winning a world computer championship of bridge). For more technical novelty, Section 6.2 extends this work to 3D GANs, adds surrogate models, and considers local convergence (see the “evolutionary” version). Section 6.3 extends it to latent diffusion models, and Section 6.4 adds Voronoi crossovers.

6.2 EG3D-cats: local and global optimization of a surrogate model

6.2.1 Context: Offline optimization of the latent variable thanks to a surrogate model. EG3D-cats [Chan et al. 2022] is a pioneering work in 3D GANs, with impressive results. In the present Section, we improve EG3D-cats by learning in the latent space: instead of randomly drawing a latent variable z , we learn a surrogate model of image quality and use it to optimize the input z to the GAN, in order to avoid z ’s leading to low quality.

Building the surrogate model. We proceed as follows:

- Generate 200 images corresponding to 200 randomly chosen latent variables z .
- Get binary user feedback: good or bad, for each image.

Table 6. Results of the AfterLearnER improvement of the EG3D-cats algorithm with human raters, using a double-blind interface with randomized left/right positioning of compared images: the percentage shows how frequently our method outperformed the vanilla LDM according to human raters.

Initial model	Proposed method	Frequency of improvement (\uparrow)	Remark
afhqcats512-128	Random search	65% (160 images)	Cats
afhqcats512-128	Evolution	71% (193 images)	Cats
ffhqrebalanced512-64		90% (180 images)	Faces

- Train a decision tree (we use the scikit-learn implementation [Pedregosa et al. 2011]) to approximate the probability, for a given latent variable z , that it generates a bad image: $tree(z) \approx P(bad|z)$.

6.2.2 **\aleph -parameter:** The latent variable z of EG3D-cats: dimension 512.

6.2.3 **\aleph -loss: The surrogate model.** We propose two variants of the algorithm, both using the trained decision tree described above to optimize the \aleph -parameter z :

- The *random search variant* applies random search on *tree*: Randomly draw z until $tree(z) = 0$, i.e., the trained decision tree predicts that the image will be ok.
- The *evolutionary version* (searching for local modifications) applies NGOpt on the objective function $l : x \mapsto tree(z_0 + \epsilon \cdot x)$ for some randomly drawn z_0 . For a small ϵ (e.g., $1e-2$), the final value is close to the starting point z_0 , thus preserving the diversity of the original GAN: this is the main advantage of the evolutionary version compared to the random search. Note that the evolutionary version works in \mathbb{R}^n and has, therefore, no theoretical guarantee of staying close to z_0 : however, it is initialized with normal random variables, and therefore the small ϵ implies that it searches in the neighborhood of z_0 first.

In both cases, we stop at a budget of 10000. To evaluate the approach, we use human raters to assess the improvement between the initial z and the optimized z . The humans (not working in the computer science field) are presented with a cat generated by EG3D-cats and a cat generated by AfterLearnER: they choose the cat image they prefer or click on “no preference”. The success rates are evaluated among cases in which they do have a preference. For the evolutionary variant, raters have to choose one of both cat images, but only images for which the initial z_0 was not satisfactory (i.e. $P(bad|z_0) > 0$) are presented: these statistical comparisons are based on paired data, i.e., z_0 vs $z_0 + \epsilon \cdot x^*$ with x^* recommended by the optimization run. Figures 4 and 5 present some qualitative results before and after the evolution done by AfterLearnER.

6.2.4 **Results: offline improvement of the model.** The results, with 4 human raters, are presented in Table 6. In all setups, we observe an improvement when using AfterLearnER compared to vanilla EG3D (i.e., all numbers are larger than 50%). The most significant improvement is seen in the enhancement of faces, with 90% of cases showing a modification. Of course, the different random seeds used for computing these statistics are distinct from those used for creating the training set of 200 images.

6.2.5 **Discussion.** We demonstrated that it is possible to learn a good approximation of the set of z ’s that lead to errors using a decision tree at a reasonable cost: labelling 200 examples is feasible for a motivated human.



Fig. 4. Example of evolution: unmodified cat (bottom) generated by EG3D-cats and its evolutionary counterpart (top). Left: the ears have been significantly improved, while the neck is improved on the right.



Fig. 5. Example of evolution: unmodified cat (bottom) generated by EG3D-cats and its evolutionary counterpart (top). In both cases, the mouth has been significantly modified, though it is still not perfect.

6.3 LDM: learning a surrogate model on 200 human feedbacks

6.3.1 *Context: Using feedback to steer the model output towards human preferences.* Latent Diffusion Models (LDM) [Rombach et al. 2022] recently provided impressive results in text-to-image generation: a prompt conditions the output. This section is based on [Videau et al. 2023], and applies the same techniques on latent models as in Section 6.2.

Building the surrogate model.

- Generate 200 images on the prompt “a photograph of an astronaut riding a horse”.
- Get a binary user feedback: good or bad, with a special emphasis on the quality of crops.
- Train a classifier to approximate the probability, for a given latent variable z , that it generates a bad image: $tree(z) \approx P(bad|z)$.

Depending on the experiment, the classifier is a decision tree or a neural network, and we use the scikit-learn implementation in both cases [Pedregosa et al. 2011]³.

6.3.2 *\aleph -parameter.* The latent variables of LDM.

³We use `MLPClassifier(solver='lbfgs', alpha=1e-5, hidden_layer_sizes=(5, 2), random_state=1)` and `tree.DecisionTreeClassifier()`.

Table 7. Results of AfterLearnER on LDM. Between parenthesis the number of rated images. The overall comparison LDM vs. AfterLearnER+LDM is statistically significant, with p-value 0.04 for Fisher’s exact test. The ‘satisfaction rate’ is described in Section 6.3.3. The p-value (Section 4.2.4) for the difference between LDM (2.9% on 486 runs) and the average case (5.7% on 382 runs) is p-val= 0.02.

Experimental setup	Optimizer	Loss	Satisfaction rate (↑)
LDM			2.9% (486)
LDM+AfterLearnER	Random search	Decision tree	5.1 % (98)
LDM+AfterLearnER	Lengler	Decision tree	5.6 % (180)
LDM+AfterLearnER	Discrete(1 + 1)	Neural net	6.7 % (104)
Average LDM+AfterLearnER			5.7 % (382)

6.3.3 **\aleph -loss: The Surrogate Model.** As in Section 6.2.1, we use the trained decision tree as AfterLearnER \aleph -loss to determine an optimal latent value z that minimizes $tree(z) \approx P(bad|z)$. The optimization is stopped as soon as it reaches some z satisfying $tree(z) = 0$.

To assess the effectiveness of this approach, we rely on human raters. Specifically, raters are asked: “Is the crop of this image of top quality and does it include the entire astronaut and horse?” We refer to this evaluation metric as the ‘satisfaction rate’.

6.3.4 **Results.** The training is done on images labeled by us, and the performance is measured on other generated images with/without AfterLearner, with different seeds. The human raters, in randomized order among the 4 tested methods, work in double-blind. The prompt is “A photograph of an astronaut riding a horse”. The results are presented in Table 7. We observe progress in all contexts: the frequency of poorly cropped images dramatically decreases.

6.3.5 **Discussion:** This success looks surprising: how can we learn something with 200 examples, whereas the latent space has dimension $4 \cdot 64 \cdot 64 = 16384$? Nevertheless, the results presented in the next Section will confirm these results, switching to an online context, with an even lower budget.

6.4 LDM with online human feedback, learning from 15 images

6.4.1 **Context:** In order to double-check the results above (successful inference from a few data points in a huge latent space), we perform the following experiment:

- 15 images are generated with the same text input.
- The users select their five favorite images.
- Learning a “local” surrogate model on the fly: these (at most 5) favorite images are separated from the other 10, using scikit-learn neural network.
- Similarly to both previous sections, we minimize the probability of generating bad images (according to the local surrogate model) using Nevergrad (Lengler algorithm [Doerr et al. 2019]), with an initial point created by crossover based on the favorite images as parents (as proposed in [Videau et al. 2023] and as detailed below).

Application of the crossover operator for 2 parents. The vanilla optimization by Nevergrad is here improved by creating a starting point for the optimization run built using a specific crossover operator, so-called Voronoi crossover [Hamda et al. 2002; Pehlivanoglu 2012; Seo and Moon 2002; Seo et al. 2005; Videau et al. 2023], in order to provide a better merging between different individuals than by geometric averages: the Voronoi split between z_1 and z_2 for getting a child corresponding to a

Algorithm 4 Pseudo-code for the crossover of images with latent variables z_1 and z_2 , at points p_1 and p_2 . Here, the user has selected the point p_1 in the image generated from the latent variable z_1 and the point p_2 in the image generated from the latent variable z_2 , out of 15 images. Latent variables are tensors with shape $64 \times 64 \times 4$.

Require: Latent variables z_1 and z_2 , coordinates $p_1 \in I_1 = LDM(z_1)$ and $p_2 \in I_2 = LDM(z_2)$.
 Create a new latent variable z of same shape as z_1 and z_2 .

```

for each  $p$  spatial coordinate in  $z$ . do
  if  $\|p_1 - p\| < \|p_2 - p\|$  then
     $z(p) = z_1(p)$ 
  else
     $z(p) = z_2(p)$ 
  end if
end for

```

crossover between images with latent variables z_1 and z_2 (Algorithm 4). These Voronoi combinations are used as starting points for the optimization by AfterLearnER.

Application of the crossover operator for more than 2 clicks by users. Two modifications of Algorithm 4 are needed. First, we might have more than 2 images chosen by the user, so we extend Algorithm 4 to more than two images. Second, we need to create more than one offspring, so that randomization is necessary. For these two extensions, we follow [Videau et al. 2023]: let us consider k clicks, with positions p_1, \dots, p_k , in images built on latent variables z_{i_1}, \dots, z_{i_k} . Each offspring image $I_{Voronoi} = G(z_{Voronoi})$ is built by constructing a latent variable $z_{Voronoi}$ as in Figures 3-5.

$$r \quad \text{is randomly drawn uniformly in } [1, 2] \quad (3)$$

$$z_{Voronoi}(x) = z_{i_j}(x) \text{ if } \forall u \neq j, \|x - p_j\| < \frac{1}{r} \|x - p_u\| \quad (4)$$

$$z_{Voronoi}(x) \sim \mathcal{N}(0, 1) \text{ for each channel otherwise} \quad (5)$$

6.4.2 N-loss. To evaluate this approach, we use a specific prompt and quality criterion (see below). We generate a batch of images with the vanilla LDM, and a second batch, using AfterLearnER, after selection of the 5 best by the user.

We then compare the number of images that fit the given criterion in the initial batch (no user feedback) and in subsequent batches (i.e., with user feedback).

6.4.3 Results. AfterLearnER was tested on three different setups:

- First setup: the prompt is “A close-up photographic portrait of a young woman with colored hair”. We consider images 15 to 28, in 2 cases: first case, the user selects red hair; and second case, the user selects blue hair. Observation: the next generation by AfterLearnER + LDM have dramatically greater proportions of red hair (resp. blue hair). Results are presented in Figure 6.
- Second context: “fighting Cthulhu in the jungle”. For the second setup (Figure 7, Figure 8), we present more sophisticated experiments with celebrities fighting Cthulhu. We observe a moderate improvement, on this easy setting of very famous people: some people, like X Y (anonymized celebrity), are easier to generate in arbitrary contexts, so that the classical

Table 8. Overview of our low-budget image generation experiments. FB refers to user feedback (clicks on the preferred images inside a screen presenting a batch of images). For Figure 10 the quality is not measured by quantified metrics and the reader can compare the top 2 rows to the bottom 2 rows there.

Figure		Context	Observation
Fig. 6	Top	2nd batch, after FB on red hair in batch 1	Mostly red hair
	Bottom	2nd batch, after FB on blue hair in batch 1	All blue hair
Fig. 7	Top	Initial batch	Success 11/14
	Middle	Batch 2 after FB on batch 1	Success 12/14
	Bottom	Batch 3 after FB on batches 1 and 2	Success 13/14
Fig. 9	Top	Initial batch	Success \approx 30%
	Bottom	After FB on the 1st batch	Success \approx 71%
Fig. 10	Top	Initial batch	Low quality
	Middle	After FB on 1st batch	
	Bottom	After FB on batches 1 and 2	High quality

LDM performs well. The prompt becomes much harder for a scientist like Yann LeCun: in this harder setting, the improvement becomes much greater (Figure 9).

- Third setup, we now check that AfterLearnER can also have an impact on realism. We just ask for “Medusa” and feed AfterLearnER with the realism opinion of the user. The second batch uses preferences mentioned by the user in the first batch, then the third batch uses preferences mentioned by the user in the second batch, and so on. Each batch improves over the previous one. Within 3 batches of 14 images, we get way more realistic portraits of Medusa (Figure 10).

Results are aggregated in Table 8. They are always positive, with a clear gap in 3 out of 4 contexts.

6.4.4 Discussion. In each setup, we increase the proportion of images that fit specific criteria. This approach is particularly effective for generating images that are difficult to produce by default, such as “Yann LeCun fighting tentacles in the Jungle.” In these challenging scenarios, the text-to-image model struggles to combine elements like Yann LeCun, a jungle, and tentacles. However, by selecting the right images, we can guide the model to produce outputs that better match user preferences, showing the effectiveness of the proposed approach.

7 OVERVIEW AND DISCUSSION

7.1 Overview

All results in the present paper come from applying AfterLearnER after a classical ML pipeline.

Depth sensing (Section 5.1): We use the small MiDaS model and optimize \mathcal{N} -parameters on a small dataset. More precisely, 300 images are used for optimizing \mathcal{N} -parameters by distillation of the big MiDaS model so that we get test errors better than the original Small MiDaS, or even (in some cases) the Hybrid MiDaS. These results only require 50 scalars of feedback for adapting a model to different loss functions. In this benchmark, the loss is not differentiable either.



The user selects red hair. Images 15 to 28, after a warm up of 14 images.



The user selects blue hair. Images 15 to 26, after a warm up of 14 images.

Fig. 6. LDM with prompt “A close up photographic portrait of a young woman with colored hair”. We present generated images, after a warm up over 14 images. The only difference between top and bottom is that the user clicks differently during the first batch. We observe variations in the necklaces and eyes when the rest of the image looks similar. In spite of the very low budget (the human user provides feedback on 14 images only) there is a clear increase in the target hair color.

Speech resynthesis (Section 5.2): We use the checkpoint previously tuned in [Kharitonov et al. 2022] and optimize two \mathcal{N} -parameter on 75% of the test set and check on the remaining test data. This is a simple experiment with just two constants, hardcoded in the original code, optimized on a small dataset. The numbers are not directly comparable to the original work as we use a split of the test set: but we show that a small feedback (40 scalars) on a split of the test set is enough for, on average, an improvement on the rest of the test set. Compared to [Ranzato et al. 2016], we do a fast distribution shift and not a whole training.

Doom/Arnold (Section 5.3): In this reinforcement learning context, we use the same simulator as the one used in the original paper/code. This consistency allows for a direct comparison of our results. We observed enhanced outcomes primarily because we focused on optimizing the actual objective function.

Transcoder (Section 5.4): We use the same training/validation data as in the GitHub repository of [Roziere et al. 2020]. We immediately observe an improvement (Figure 3) only using a few hundred scalars. We do not use any information about the objective function, so we could have an online estimator such as speed, memory consumption or elegance — which cannot be done with the original supervised learning.

Interactive GAN (Section 6.1): The results here are close to those in [Rozière et al. 2020], but obtained faster using discrete optimization [Doerr et al. 2019] and tools [Videau et al. 2023], and we improved diversity by optimizing the initialization as in Algorithm 3. Experimental results show that eight clicks are sufficient for most cases, with three clicks (on average) for our chosen classes.



First batch of 14 images. Tentacles: in 11 images. XY is the only human: in 12 images.



Second batch of 14 images. Tentacles in 12 images. XY is the only human: in all images.



Third batch of 14 images. Tentacles: in 13 images. XY is the only human: in all images.

Fig. 7. XXX YYY (anonymized) fighting tentacles in the jungle. The original LDM is already good here, but we observe an increased frequency of XXX YYY and an increased frequency of tentacles in the new batches. A more challenging task is proposed in Figure 9.



Fig. 8. XY (anonymized) fighting tentacles in the jungle, selection of best images, less than 50 runs of LDM, one minute per LDM run with default parameters on a Mac M1.

3D Gan EG3D for AFHQ (cats) (Section 6.2): With 200 feedbacks, we built a more realistic EG3D-cats, outperforming state-of-the-art in three-dimensional cats and three-dimensional face generation.

LDM (Section 6.3) : We provide an interactive counterpart of LDM. The fact that it works is quite counter-intuitive: the latent space has dimension $4 \cdot 64 \cdot 64$. We perform several tests with hair color, image quality, and realism, and results are repeatedly confirmed. They are in line with user



Initial generations of 15 images, by the vanilla LDM code. Tentacles in 4 or 5 images, over 15: tentacles are difficult to obtain when a scientist is in the picture.



After selection of the 5 preferred images out of the 15 above, 14 new generations by AfterLearnER. Tentacles in 10/14 images.

Fig. 9. A scientist fighting tentacles in the jungle. The frequency of tentacles has increased a lot. All images have significant differences in terms of position. We observe again that 15 images evaluated by the user are enough for a meaningful impact.

needs: whereas most LDM users (in particular in the new field of prompt engineering for txt2img) do many independent rerolls, we guide these rerolls using previous results. Section 6.4 presents results in a very low budget case.

7.2 Discussion

Before detailing the experimental validation, we take a look at the a priori benefits of retrofitting on the problems described in Table 2, according to the rationale developed in Section 3.3.

Table 2 shows, in particular, the different sizes of the feedback used in the following. It can always be provided by humans or computationally expensive solvers. Regarding RLHF (Reinforcement Learning with Human Feedback – such as EG3D, LDM, Facial Composites), we consider feedback limited to dozens or hundreds of scalars (far less than most works as discussed in Section 2.2.1).

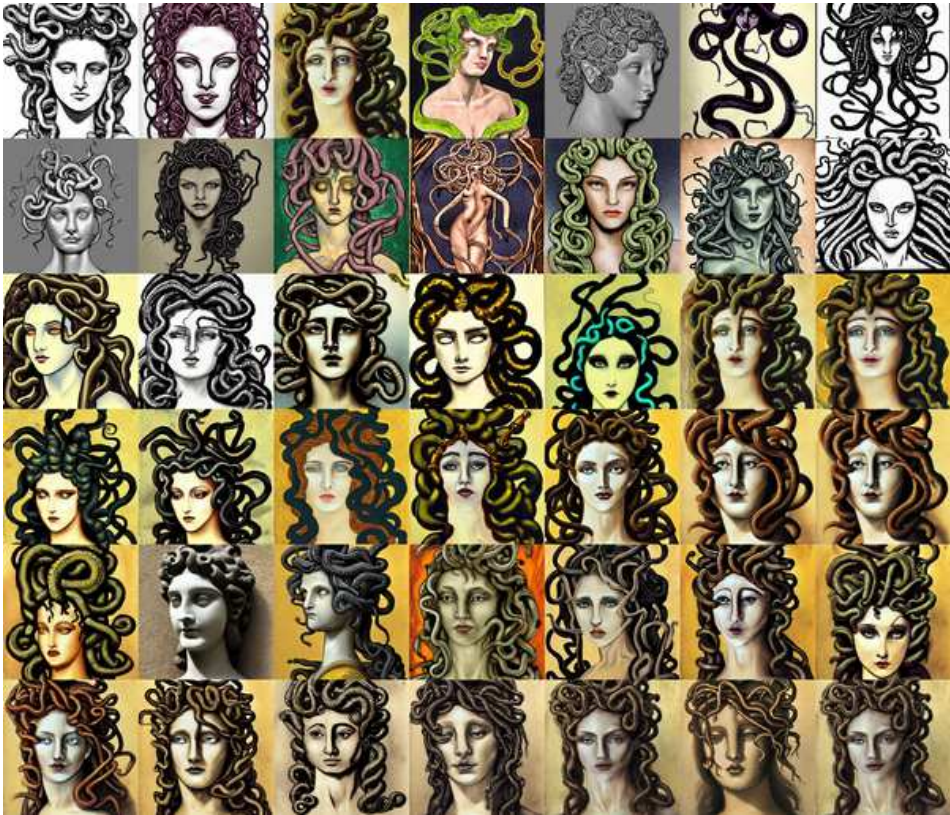


Fig. 10. Medusa. Top two rows: first batch, i.e., equivalent to default LDM. Rows 3 and 4: second generation, after clicking on the most realistic image of the first batch. Rows 5 and 6: generation 3, after clicking on the two most realistic images of generation 2. Colors become better, and sub-sternal dimples appear. We observe that a user feedback about 2 generations of images are enough for improving outputs.

For facial composites (Section 6.1), speech re-synthesis (Section 5.2) and depth sensing (Section 5.1), the number of runs is $k = 1$ because of the computational cost (for depth and speech) or limited human attention span (for facial composites and latent diffusion models).

Our approach requires less data and utilizes feedback at a more aggregated level, compared to most RLHF [Zhu et al. 2023] and Human In The Loop Reinforcement Learning (HITLRL [Arakawa et al. 2018]) approaches. Specifically, our approach needs only one objective function value per parametrized model and dataset. In contrast, classical stochastic-gradient methods require one objective function value and one gradient value per parameterized model and per data point. The process is hence compatible with evaluation by humans, who can study an entire system output, and compare on key points (see e.g., human feedback for interactive GAN Section 6.1), or with end-of-episode (delayed) evaluations by complex simulators (e.g., VizDoom [Kempka et al. 2016] for Doom, in Section 5.3) or non-differentiable computational accuracy (in code translation, Section 5.4).

8 CONCLUSIONS

This paper demonstrates the potential of integrating small-scale feedback directly into the optimization process, as in retrofitting, through black-box optimization approaches. Likewise, such a strategy

is especially beneficial for optimizing a few scalars using a non-differentiable criterion, a common challenge in various fields. That way, we provide substantial improvements in state-of-the-art Deep Learning (DL) applications, e.g., use cases such as Doom and code translation. Furthermore, our methodology enables the generation of facial composites with minimal user interaction, requiring as few as three interactions for getting a first approximation. Similarly, we optimize \aleph -parameters for depth estimation, language translation, and speech synthesis. Our method requires only dozens to hundreds of (e.g., human) evaluations to achieve significant improvements. Additionally, we have enhanced the EG3D-cats model with a streamlined codebase, illustrating our approach’s versatility and practicality (see Algorithm 8 in appendix F). Overall, our findings underscore the value of human-in-the-loop methodologies or simulation-based feedbacks in refining DL solutions across various domains without relying on thousands of feedbacks.

We make the following recommendations for the use of AfterLearnER:

- Consider problems in which the actual objective is not differentiable and is hence typically approximated for gradient-based training by various proxies, or by ad-hoc reward shaping.
- Apply AfterLearnER *after* the classical gradient-based training, and without any backprop retraining.
- Restrict the \aleph -parameter to key parameters: typically, some parameters at the input or output transformations, or a single layer, as small as possible. Dimensions in the 1000s is manageable in a black-box manner (though this, of course, depends on the budget), but we prefer as much as possible small families of parameters that intersect all paths from input to output.
- Increasing the number of runs (parameter k), or the parallelism λ , makes the code closer to random search, and less prone to overfitting, as predicted by the theoretical analysis of Section 3.3.2 and confirmed in the experiments.

We emphasize the concept of small aggregated anytime feedback (Section 3.3.4). While we did a part of our experiments from automatically computed feedback (e.g., word error rate based on programs for speech synthesis or the biggest MiDaS model in depth estimation), AfterLearnER uses an aggregated feedback, which could be provided by humans or expensive simulators, based on a global experience of the system, without the need for fine grain feedback. Also, this shows a clear generalization: compared to systems using millions of fine-grained feedbacks, our system can not so easily “cheat” (overfit) using redundancies between train/validation and testing.

Limitations and further work

Most of the feature construction was performed by DL: what we propose can be added on top of a DL solution, but does not replace it. We outperform Arnold for Doom, but only with Arnold and its reward shaping as an excellent starting point. The situation is similar for speech resynthesis, interactive generation, and depth sensing. In the case of the Transcoder, we manage to optimize a few weights of the checkpoint within a few dozen evaluations.

Maybe some of our results could be improved by applying AfterLearnER on several layers in turn: in the present paper, we only heuristically guessed which parameters to optimize and did not investigate larger search spaces. This might be particularly true for cases in which we can generate new data with a simulator, as in the case of Doom (Section 5.3).

Improving generalization by searching for flat optima is a challenging topic [Baldassi et al. 2020; He et al. 2019; Hoffer et al. 2017], mostly explored for gradient-based optimization of weights: our context (black-box optimization, validation set, after training) is specific, promising, and deserves exploration. This includes the theory in Section 3.3.2.

Multi-objective extensions seem to be natural for Arnold/Doom (using the various reward shaping criteria used in the original code) and for code translation, where BLEU and comp. acc.

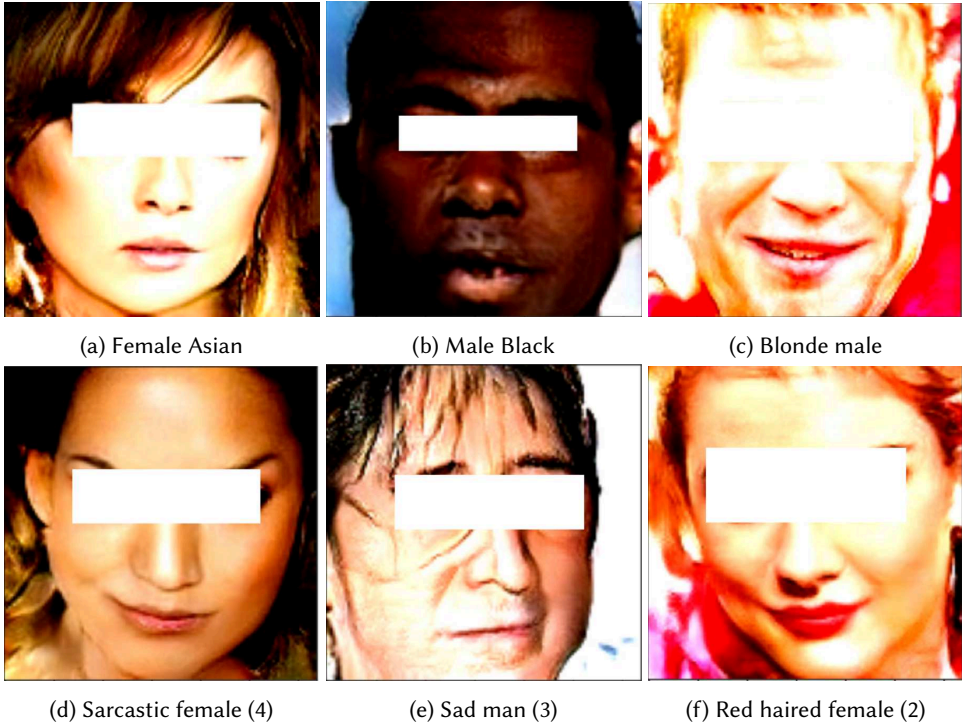


Fig. 11. First 3 images (top, and middle left): examples corresponding to female Asian, male black, and blonde male, respectively, i.e., 3 categories used in our experiment. The 3 other images are test cases with labels not provided in the tuning in Algorithm 3: they show the versatility of the method. The number in parentheses is the number of clicks before obtaining the result. None of the faces presented here corresponds to a real-world person: these faces are obtained by optimization through Algorithm 2.

are completely different measures, and for the many criteria of depth sensing: there exist many multi-objective variants of black-box optimizers.

The present paper demonstrated the applicability of AfterLearnER, with experiments reproducible with a relatively low budget. Some obvious further works include the large-scale application on unsolved problems, such as fighting hallucinations in large language models or optimizing code translation for speed.

ACKNOWLEDGEMENTS

The authors thank the reviewers for their insightful and constructive feedback, which has substantially improved the quality of this work. AL acknowledges support from the French National Research Agency (ANR) under Grant No. ANR-23-CPJ1-0099-01.

REFERENCES

- Josh Abramson, Arun Ahuja, Federico Carnevale, Petko Georgiev, Alex Goldin, Alden Hung, Jessica Landon, Jirka Lhotka, Timothy Lillicrap, Alistair Muldal, George Powell, Adam Santoro, Guy Scully, Sanjana Srivastava, Tamara von Glehn, Greg Wayne, Nathaniel Wong, Chen Yan, and Rui Zhu. 2022. Improving Multimodal Interactive Agents with Reinforcement Learning from Human Feedback. [arXiv:2211.11602](https://arxiv.org/abs/2211.11602)
- Stephen Adams, Tyler Cody, and Peter A. Beling. 2022. A survey of inverse reinforcement learning. *Artif. Intell. Rev.* 55, 6 (aug 2022), 4307–4346.

- Riku Arakawa, Sosuke Kobayashi, Yuya Unno, Yuta Tsuboi, and Shin-ichi Maeda. 2018. Dqn-tamer: Human-in-the-loop reinforcement learning with intractable feedback. *arXiv:1810.11748* (2018).
- SME Artelys. 2015a. <https://www.artelys.com/news/159/16/KNITRO-wins-the-GECCO-2015-Black-Box-Optimization-Competition>
- SME Artelys. 2015b. Artelys SQP Wins the BBCOMP competition. <https://www.ini.rub.de/PEOPLE/glasmtbl/projects/bbcomp/index.html>.
- Filipe Assunção, Nuno Lourenço, Penousal Machado, and Bernardete Ribeiro. 2019. DENSER: Deep Evolutionary Network Structured Representation. *Genetic Programming and Evolvable Machines* 20 (03 2019).
- Noor Awad, Gresa Shala, Difan Deng, Neeratyooy Mallik, Matthias Feurer, Katharina Eggensperger, Andre' Biedenkapp, Diederick Vermetten, Hao Wang, Carola Doerr, Marius Lindauer, and Frank Hutter. 2020. Squirrel: A Switching Hyperparameter Optimizer. *arXiv:2012.08180*
- Th. Bäck, D.B. Fogel, and Z. Michalewicz (Eds.). 1997. *Handbook of Evolutionary Computation*. Oxford University Press.
- Alexei Baevski, Yuhao Zhou, Abdelrahman Mohamed, and Michael Auli. 2020. wav2vec 2.0: A framework for self-supervised learning of speech representations. *Advances in neural information processing systems* 33 (2020), 12449–12460.
- Carlo Baldassi, Enrico M. Malatesta, Matteo Negri, and Riccardo Zecchina. 2020. Wide flat minima and optimal generalization in classifying high-dimensional Gaussian mixtures. *arXiv:2010.14761* (2020).
- David Berthelot, Tom Schumm, and Luke Metz. 2017. BEGAN: Boundary Equilibrium Generative Adversarial Networks. *CoRR abs/1703.10717* (2017). *arXiv:1703.10717*
- Hans-Georg Beyer. 1998. Mutate large, but inherit small! On the analysis of rescaled mutations in $(1, \lambda)$ -ES with noisy fitness data. In *Parallel Problem Solving from Nature — PPSN V*. Springer, 109–118.
- Reiner Birkel, Diana Wofk, and Matthias Müller. 2023. Midas v3. 1—a model zoo for robust monocular relative depth estimation. *arXiv:2307.14460* (2023).
- Carlo Bonferroni. 1936. Teoria statistica delle classi e calcolo delle probabilita. *Pubblicazioni del R Istituto Superiore di Scienze Economiche e Commerciali di Firenze* 8 (1936), 3–62.
- Philip Bontrager, Wending Lin, Julian Togelius, and Sebastian Risi. 2018. Deep Interactive Evolution. *7th International Conference on Computational Intelligence in Music, Sound, Art and Design* (2018).
- Rebekka Burkholz. 2024. Batch normalization is sufficient for universal function approximation in CNNs. In *The 12th International Conference on Learning Representations*.
- Marie-Liesse Cauwet and Olivier Teytaud. 2016. Noisy Optimization: Fast Convergence Rates with Comparison-Based Algorithms. In *Genetic and Evolutionary Computation Conference*. 1101–1106.
- Eric R. Chan, Connor Z. Lin, Matthew A. Chan, Koki Nagano, Boxiao Pan, Shalini De Mello, Orazio Gallo, Leonidas Guibas, Jonathan Tremblay, Sameh Khamis, Tero Karras, and Gordon Wetzstein. 2022. Efficient Geometry-aware 3D Generative Adversarial Networks. In *CVPR*.
- Dian Chen, Dequan Wang, Trevor Darrell, and Sayna Ebrahimi. 2022. Contrastive Test-Time Adaptation. In *IEEE/CVF Conference on Computer Vision and Pattern Recognition*. 295–305.
- Billy Chiu, Simon Baker, Martha Palmer, and Anna Korhonen. 2019. Enhancing biomedical word embeddings by retrofitting to verb clusters. In *BioNLP@ACL*.
- Shih-Yuan Chiu, Ching-Nung Lin, Jialin Liu, Tsang-Cheng Su, Fabien Teytaud, Olivier Teytaud, and Shi-Jim Yen. 2015. Differential Evolution for Strongly Noisy Optimization: Use 1.01^n Resamplings at Iteration n and Reach the $-1/2$ Slope. In *IEEE Congress on Evolutionary Computation*.
- Duc-Cuong Dang and Per Kristian Lehre. 2016. Self-adaptation of Mutation Rates in Non-elitist Populations. In *Parallel Problem Solving from Nature - PPSN XIV - 14th International Conference*. 803–813.
- Richard Dawson. 2007. Re-engineering cities: a framework for adaptation to global change. *Philosophical Transactions of the Royal Society A: Mathematical, Physical and Engineering Sciences* 365, 1861 (2007), 3085–3098.
- Tim Dixon and Malcolm Eames. 2013. Scaling up: the challenges of urban retrofit. *Building research & information* 41, 5 (2013), 499–503.
- Benjamin Doerr, Carola Doerr, and Johannes Lengler. 2019. Self-Adjusting Mutation Rates with Provably Optimal Success Rules. In *Genetic and Evolutionary Computation Conference*. 1479–1487.
- James Douglas. 2006. *Building adaptation*. Routledge.
- A. E. Eiben and James E. Smith. 2015. *Introduction to Evolutionary Computing, Second Edition*. Springer.
- Hafsteinn Einarsson, Marcelo Matheus Gauy, Johannes Lengler, Florian Meier, Asier Mujika, Angelika Steger, and Felix Weissenberger. 2019. The linear hidden subset problem for the $(1+1)$ -EA with scheduled and adaptive mutation rates. *Theoretical Computer Science* 785 (2019), 150–170.
- Manaal Faruqui, Jesse Dodge, Sujay Kumar Jauhar, Chris Dyer, Eduard Hovy, and Noah A. Smith. 2015a. Retrofitting Word Vectors to Semantic Lexicons. In *Conference of the North American Chapter of the Association for Computational Linguistics: Human Language Technologies*, Rada Mihalcea, Joyce Chai, and Anoop Sarkar (Eds.). 1606–1615.

- Manaal Faruqui, Jesse Dodge, Sujay Kumar Jauhar, Chris Dyer, Eduard Hovy, and Noah A. Smith. 2015b. Retrofitting Word Vectors to Semantic Lexicons. In *Conference of the North American Chapter of the Association for Computational Linguistics: Human Language Technologies*, Rada Mihalcea, Joyce Chai, and Anoop Sarkar (Eds.), 1606–1615.
- Matthias Feurer and Frank Hutter. 2019. Hyperparameter optimization. In *Automated Machine Learning: Methods, Systems, Challenges*, Frank Hutter, Lars Kotthoff, and Joaquin Vanschoren (Eds.), 3–38.
- Hervé Fournier and Olivier Teytaud. 2011. Lower Bounds for Comparison Based Evolution Strategies Using VC-dimension and Sign Patterns. *Algorithmica* 59, 3 (2011), 387–408.
- Angeliki Giannou, Shashank Rajput, and Dimitris Papailiopoulos. 2023. The Expressive Power of Tuning Only the Normalization Layers. In *The 36th Annual Conference on Learning Theory*, Gergely Neu and Lorenzo Rosasco (Eds.), Vol. 195, 4130–4131.
- Fred Glover and Manuel Laguna. 1997. *Tabu Search*. Kluwer Academic Publishers.
- David E. Goldberg. 1989. *Genetic Algorithms in Search, Optimization and Machine Learning*. Addison-Wesley.
- Sachin Goyal, Mingjie Sun, Aditi Raghunathan, and J. Zico Kolter. 2022. Test Time Adaptation via Conjugate Pseudo-labels. In *Advances in Neural Information Processing Systems*, S. Koyejo, S. Mohamed, A. Agarwal, D. Belgrave, K. Cho, and A. Oh (Eds.), Vol. 35, 6204–6218.
- Hatem Hamda, François Jouve, Evelyne Lutton, Marc Schoenauer, and Michele Sebag. 2002. Compact unstructured representations for evolutionary design. *Applied Intelligence* 16 (2002), 139–155.
- Nikolaus Hansen and Andreas Ostermeier. 2003. Completely Derandomized Self-Adaptation in Evolution Strategies. *Evolutionary Computation* 11, 1 (2003).
- Haowei He, Gao Huang, and Yang Yuan. 2019. Asymmetric Valleys: Beyond Sharp and Flat Local Minima. In *Advances in Neural Information Processing Systems*, H. Wallach, H. Larochelle, A. Beygelzimer, F. d'Alché-Buc, E. Fox, and R. Garnett (Eds.), Vol. 32.
- Verena Heidrich-Meisner and Christian Igel. 2009. Hoeffding and Bernstein Races for Selecting Policies in Evolutionary Direct Policy Search. In *Proceedings of the 26th Annual International Conference on Machine Learning (ICML '09)*. ACM, 401–408.
- Gaurush Hiranandani, Hari Narasimhan, Jatin Mathur, Mahdi Milani Fard, and Sanmi Koyejo. 2021. Optimizing Blackbox Metrics with Iterative Example Weighting. In *38th International Conference on Machine Learning*.
- Elad Hoffer, Itay Hubara, and Daniel Soudry. 2017. Train Longer, Generalize Better: Closing the Generalization Gap in Large Batch Training of Neural Networks. In *31st International Conference on Neural Information Processing Systems*, 1729–1739.
- John H. Holland. 1975. *Adaptation in Natural and Artificial Systems*. University of Michigan Press.
- Neil Houlsby, Andrei Giurgiu, Stanislaw Jastrzebski, Bruna Morrone, Quentin De Laroussilhe, Andrea Gesmundo, Mona Attariyan, and Sylvain Gelly. 2019. Parameter-efficient transfer learning for NLP. In *International Conference on Machine Learning*, 2790–2799.
- Edward J Hu, Yelong Shen, Phillip Wallis, Zeyuan Allen-Zhu, Yanzhi Li, Shean Wang, Lu Wang, and Weizhu Chen. 2021. Lora: Low-rank adaptation of large language models. *arXiv:2106.09685* (2021).
- Chen Huang, Shuangfei Zhai, Pengsheng Guo, and Josh Susskind. 2021. MetricOpt: Learning To Optimize Black-Box Evaluation Metrics. In *IEEE/CVF Conference on Computer Vision and Pattern Recognition*, 174–183.
- Seung-Jun Hwang, Sung-Jun Park, Gyu-Min Kim, and Joong-Hwan Baek. 2021. Unsupervised Monocular Depth Estimation for Colonoscopy System Using Feedback Network. *Sensors* 21, 8 (2021).
- Ashesh Jain, Shikhar Sharma, Thorsten Joachims, and Ashutosh Saxena. 2015. Learning preferences for manipulation tasks from online coactive feedback. *Int. J. Robotics Res.* 34, 10 (2015), 1296–1313.
- Qijia Jiang, Olaoluwa Adigun, Harikrishna Narasimhan, Mahdi Milani Fard, and Maya Gupta. 2020. Optimizing Black-box Metrics with Adaptive Surrogates. In *37th International Conference on Machine Learning*, Hal Daumé III and Aarti Singh (Eds.), Vol. 119, 4784–4793.
- Mingsheng Jiao, Tingrui Yu, Xuan Li, Guanjie Qiu, Xiaodong Gu, and Beijun Shen. 2023. On the Evaluation of Neural Code Translation: Taxonomy and Benchmark. *arXiv:2308.08961*
- Kirthevasan Kandasamy, Willie Neiswanger, Jeff Schneider, Barnabás Póczos, and Eric P. Xing. 2018. Neural architecture search with Bayesian optimisation and optimal transport. In *32nd International Conference on Neural Information Processing Systems*, Samy Bengio, Hanna M. Wallach, Hugo Larochelle, Kristen Grauman, and Nicolò Cesa-Bianchi (Eds.), 2020–2029.
- Tero Karras, Timo Aila, Samuli Laine, and Jaakko Lehtinen. 2018. Progressive Growing of GANs for Improved Quality, Stability, and Variation. In *Proceedings of ICLR*.
- Michał Kempka, Marek Wydmuch, Grzegorz Runc, Jakub Toczek, and Wojciech Jaśkowski. 2016. ViZDoom: A Doom-based AI Research Platform for Visual Reinforcement Learning. *arXiv:1605.02097* (2016).
- James Kennedy and Russell C. Eberhart. 1995. Particle swarm optimization. In *IEEE International Conference on Neural Networks*, 1942–1948.

- Vasil Khalidov, Maxime Oquab, Jérémy Rapin, and Olivier Teytaud. 2019. Consistent population control: generate plenty of points, but with a bit of resampling. In *15th ACM/SIGEVO Conference on Foundations of Genetic Algorithms*. 116–123.
- Eugene Kharitonov, Jade Copet, Kushal Lakhotia, Tu Anh Nguyen, Paden Tomasello, Ann Lee, Ali Elkahky, Wei-Ning Hsu, Abdelrahman Mohamed, Emmanuel Dupoux, and Yossi Adi. 2022. textless-lib: a Library for Textless Spoken Language Processing. *arXiv:2202.07359* (2022).
- Changyeon Kim, Jongjin Park, Jinwoo Shin, Honglak Lee, Pieter Abbeel, and Kimin Lee. 2023. Preference Transformer: Modeling Human Preferences using Transformers for RL. In *The 11th International Conference on Learning Representations*.
- S. Kirkpatrick, C. D. Gelatt, and M. P. Vecchi. 1983. Optimization by Simulated Annealing. 220, 4598 (1983), 671–680.
- Guillaume Lample and Devendra Singh Chaplot. 2017. Playing FPS Games with Deep Reinforcement Learning. In *Thirty-First AAAI Conference on Artificial Intelligence*. 2140–2146.
- J. Lee, D. Das, J. Choo, and S. Choi. 2023a. Towards Open-Set Test-Time Adaptation Utilizing the Wisdom of Crowds in Entropy Minimization. In *IEEE/CVF International Conference on Computer Vision*. 16334–16334.
- Kimin Lee, Hao Liu, Moonkyung Ryu, Olivia Watkins, Yuqing Du, Craig Boutilier, Pieter Abbeel, Mohammad Ghavamzadeh, and Shixiang Shane Gu. 2023b. Aligning Text-to-Image Models using Human Feedback. *arXiv:2302.12192*
- Zhengqi Li, Tali Dekel, Forrester Cole, Richard Tucker, Noah Snaveley, Ce Liu, and William T. Freeman. 2019. Learning the Depths of Moving People by Watching Frozen People. In *Proceedings of the IEEE Conference on Computer Vision and Pattern Recognition (CVPR)*.
- Vladislav Lialin, Vijeta Deshpande, and Anna Rumshisky. 2023. Scaling down to scale up: A guide to parameter-efficient fine-tuning. *arXiv:2303.15647* (2023).
- Jialin Liu, Antoine Moreau, Mike Preuss, Jeremy Rapin, Baptiste Roziere, Fabien Teytaud, and Olivier Teytaud. 2020. Versatile Black-Box Optimization. In *Genetic and Evolutionary Computation Conference*. 620–628.
- Shih-Yang Liu, Chien-Yi Wang, Hongxu Yin, Pavlo Molchanov, Yu-Chiang Frank Wang, Kwang-Ting Cheng, and Min-Hung Chen. 2024. Dora: Weight-decomposed low-rank adaptation. *arXiv:2402.09353* (2024).
- Kevin Lu, Aditya Grover, Pieter Abbeel, and Igor Mordatch. 2022. Frozen Pretrained Transformers as Universal Computation Engines. *AAAI Conference on Artificial Intelligence* 36, 7 (Jun. 2022), 7628–7636.
- Fangchang Ma and Sertac Karaman. 2018. Sparse-to-dense: Depth prediction from sparse depth samples and a single image. In *IEEE international conference on robotics and automation*. 4796–4803.
- Laurent Meunier, Herilalaina Rakotoarison, Pak-Kan Wong, Baptiste Roziere, Jérémy Rapin, Olivier Teytaud, Antoine Moreau, and Carola Doerr. 2022a. Black-Box Optimization Revisited: Improving Algorithm Selection Wizards Through Massive Benchmarking. *IEEE Trans. Evol. Comput.* 26, 3 (2022), 490–500.
- Laurent Meunier, Herilalaina Rakotoarison, Pak Kan Wong, Baptiste Roziere, Jérémy Rapin, Olivier Teytaud, Antoine Moreau, and Carola Doerr. 2022b. Black-Box Optimization Revisited: Improving Algorithm Selection Wizards Through Massive Benchmarking. *IEEE Transactions on Evolutionary Computation* 26, 3 (2022), 490–500.
- Mehdi Mirza and Simon Osindero. 2014. Conditional generative adversarial nets. *arXiv preprint arXiv:1411.1784* (2014).
- Rémi Munos. 2014. *From Bandits to Monte-Carlo Tree Search: The Optimistic Principle Applied to Optimization and Planning*. Technical Report.
- Shuaicheng Niu, Jiayang Wu, Yifan Zhang, Yaofu Chen, Shijian Zheng, Peilin Zhao, and Mingkui Tan. 2022. Efficient Test-Time Model Adaptation without Forgetting. In *39th International Conference on Machine Learning*, Kamalika Chaudhuri, Stefanie Jegelka, Le Song, Csaba Szepesvari, Gang Niu, and Sivan Sabato (Eds.), Vol. 162. 16888–16905.
- Shuaicheng Niu, Jiayang Wu, Yifan Zhang, Zhiquan Wen, Yaofu Chen, Peilin Zhao, and Mingkui Tan. 2023. Towards Stable Test-time Adaptation in Dynamic Wild World. In *The 11th International Conference on Learning Representations*.
- Maxime Oquab, Timothée Darcet, Théo Moutakanni, Huy Vo, Marc Szafraniec, Vasil Khalidov, Pierre Fernandez, Daniel Haziza, Francisco Massa, Alaaeldin El-Nouby, et al. 2023. Dinov2: Learning robust visual features without supervision. *arXiv:2304.07193* (2023).
- Long Ouyang, Jeffrey Wu, Xu Jiang, Diogo Almeida, Carroll Wainwright, Pamela Mishkin, Chong Zhang, Sandhini Agarwal, Katarina Slama, Alex Ray, et al. 2022. Training language models to follow instructions with human feedback. *Advances in Neural Information Processing Systems* 35 (2022), 27730–27744.
- Kishore Papineni, Salim Roukos, Todd Ward, and Wei-Jing Zhu. 2002. BLEU: a method for automatic evaluation of machine translation. In *40th annual meeting on association for computational linguistics*. 311–318.
- Sandip Paul, Bhuvan Jhamb, Deepak Mishra, and M. Senthil Kumar. 2022. Edge loss functions for deep-learning depth-map. *Machine Learning with Applications* 7 (2022), 100218.
- Fabian Pedregosa, Gaël Varoquaux, Alexandre Gramfort, Vincent Michel, Bertrand Thirion, Olivier Grisel, Mathieu Blondel, Peter Prettenhofer, Ron Weiss, Vincent Dubourg, Jake Vanderplas, Alexandre Passos, David Cournapeau, Matthieu Brucher, Matthieu Perrot, and Édouard Duchesnay. 2011. Scikit-learn: Machine Learning in Python. *Journal of Machine Learning Research* 12 (2011), 2825–2830.
- Y. Volkan Pehlivanoglu. 2012. A new vibrational genetic algorithm enhanced with a Voronoi diagram for path planning of autonomous UAV. *Aerospace Science and Technology* 16, 1 (2012), 47–55.

- Adam Polyak, Yossi Adi, Jade Copet, Eugene Kharonov, Kushal Lakhota, Wei-Ning Hsu, Abdelrahman Mohamed, and Emmanuel Dupoux. 2021. Speech Resynthesis from Discrete Disentangled Self-Supervised Representations. *arXiv:2104.00355* (2021).
- Michael J.D. Powell. 1964. An efficient method for finding the minimum of a function of several variables without calculating derivatives. *Comput. J.* 7, 2 (1964), 155–162.
- Michael J.D. Powell. 1994. *A Direct Search Optimization Method That Models the Objective and Constraint Functions by Linear Interpolation*. Springer Netherlands, 51–67.
- Ryan Prenger, Rafael Valle, and Bryan Catanzaro. 2019. Waveglow: A flow-based generative network for speech synthesis. In *IEEE International Conference on Acoustics, Speech and Signal Processing*. 3617–3621.
- René Ranftl, Katrin Lasinger, David Hafner, Konrad Schindler, and Vladlen Koltun. 2022. Towards Robust Monocular Depth Estimation: Mixing Datasets for Zero-Shot Cross-Dataset Transfer. *IEEE Transactions on Pattern Analysis and Machine Intelligence* 44, 3 (2022).
- Marc’Aurelio Ranzato, Sumit Chopra, Michael Auli, and Wojciech Zaremba. 2016. Sequence Level Training with Recurrent Neural Networks. In *4th International Conference on Learning Representations*, Yoshua Bengio and Yann LeCun (Eds.).
- Jeremy Rapin and Olivier Teytaud. 2018. Nevergrad - A gradient-free optimization platform. <https://GitHub.com/FacebookResearch/Nevergrad>.
- Ingo Rechenberg. 1973. *Evolutionstrategie: Optimierung Technischer Systeme nach Prinzipien des Biologischen Evolution*. Fromman-Holzboog Verlag.
- M. Riviere. 2019. Pytorch GAN Zoo. https://GitHub.com/FacebookResearch/pytorch_GAN_zoo.
- Michal Rolinek, Vit Musil, Anselm Paulus, Marin Vlastelica, Claudio Michaelis, and Georg Martius. 2020. Optimizing Rank-Based Metrics With Blackbox Differentiation. In *IEEE/CVF Conference on Computer Vision and Pattern Recognition*.
- Robin Rombach, Andreas Blattmann, Dominik Lorenz, Patrick Esser, and Björn Ommer. 2022. High-Resolution Image Synthesis With Latent Diffusion Models. In *IEEE/CVF Conference on Computer Vision and Pattern Recognition*. 10684–10695.
- Raymond Ros and Nikolaus Hansen. 2008. A Simple Modification in CMA-ES Achieving Linear Time and Space Complexity. In *Parallel Problem Solving from Nature – PPSN X*. Springer Berlin Heidelberg, 296–305.
- David Rozado. 2023. RightWingGPT – An AI Manifesting the Opposite Political Biases of ChatGPT. <https://davidrozado.substack.com/p/rightwinggpt> Last accessed on August 2024.
- Baptiste Roziere, Marie-Anne Lachaux, Lowik Chausson, and Guillaume Lample. 2020. Unsupervised translation of programming languages. *Advances in Neural Information Processing Systems* 33 (2020), 20601–20611.
- Baptiste Roziere, Fabien Teytaud, Vlad Hosu, Hanhe Lin, Jérémy Rapin, Mariia Zameshina, and Olivier Teytaud. 2020. EvolGAN: Evolutionary Generative Adversarial Networks. In *15th Asian Conference on Computer Vision (Lecture Notes in Computer Science, Vol. 12625)*, Hiroshi Ishikawa, Cheng-Lin Liu, Tomás Pajdla, and Jianbo Shi (Eds.). 679–694.
- Tim Salimans, Jonathan Ho, Xi Chen, Szymon Sidor, and Ilya Sutskever. 2017. Evolution strategies as a scalable alternative to reinforcement learning. *arXiv:1703.03864* (2017).
- H.-P. Schwefel. 1995. *Numerical Optimization of Computer Models* (2nd ed.). John Wiley & Sons.
- Dong-il Seo and Byung Ro Moon. 2002. Voronoi Quantized Crossover For Traveling Salesman Problem. In *GECCO 2002: Proceedings of the Genetic and Evolutionary Computation Conference, New York, USA, 9-13 July 2002*, William B. Langdon, Erick Cantú-Paz, Keith E. Mathias, Rajkumar Roy, David Davis, Riccardo Poli, Karthik Balakrishnan, Vasant G. Honavar, Günter Rudolph, Joachim Wegener, Larry Bull, Mitchell A. Potter, Alan C. Schultz, Julian F. Miller, Edmund K. Burke, and Natasa Jonoska (Eds.). Morgan Kaufmann, 544–552.
- Jeong-Yeon Seo, Sang-Min Park, Seoung Soo Lee, and Deok-Soo Kim. 2005. Regrouping Service Sites: A Genetic Approach Using a Voronoi Diagram. In *Computational Science and Its Applications – ICCSA 2005*, Osvaldo Gervasi, Marina L. Gavrilova, Vipin Kumar, Antonio Laganá, Heow Pueh Lee, Youngsong Mun, David Taniar, and Chih Jeng Kenneth Tan (Eds.). Springer Berlin Heidelberg, Berlin, Heidelberg, 652–661.
- Joar Skalse, Nikolaus H. R. Howe, Dmitrii Krasheninnikov, and David Krueger. 2023. Defining and characterizing reward hacking. In *36th International Conference on Neural Information Processing Systems*.
- Dennis J. N. J. Soemers, Vegard Mella, Eric Piette, Matthew Stephenson, Cameron Browne, and Olivier Teytaud. 2023. Towards a General Transfer Approach for Policy-Value Networks. *Transactions on Machine Learning Research* (2023).
- Robyn Speer, Joshua Chin, and Catherine Havasi. 2017. Conceptnet 5.5: An open multilingual graph of general knowledge. In *AAAI Conference on Artificial Intelligence*, Vol. 31.
- Rainer Storn and Kenneth Price. 1997. Differential Evolution - A Simple and Efficient Heuristic for Global Optimization over Continuous Spaces. *J. of Global Optimization* 11, 4 (Dec. 1997), 341–359.
- Thomas Stützle and Rubén Ruiz. 2018. Iterated Local Search. In *Handbook of Heuristics*, Rafael Martí, Panos M. Pardalos, and Mauricio G. C. Resende (Eds.). Springer, 579–605.
- Tianxiang Sun, Yunfan Shao, Hong Qian, Xuanjing Huang, and Xipeng Qiu. 2022. Black-Box Tuning for Language-Model-as-a-Service. In *39th International Conference on Machine Learning*, Kamalika Chaudhuri, Stefanie Jegelka, Le Song, Csaba Szepesvari, Gang Niu, and Sivan Sabato (Eds.), Vol. 162. 20841–20855.

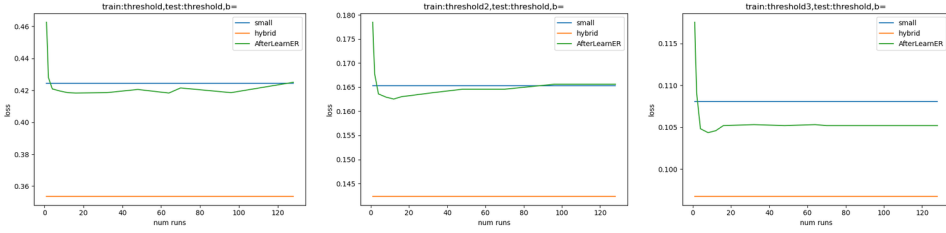
- Yu Sun, Xiaolong Wang, Zhuang Liu, John Miller, Alexei Efros, and Moritz Hardt. 2020. Test-Time Training with Self-Supervision for Generalization under Distribution Shifts. In *37th International Conference on Machine Learning*, Hal Daumé III and Aarti Singh (Eds.), Vol. 119. 9229–9248.
- André Susano Pinto, Alexander Kolesnikov, Yuge Shi, Lucas Beyer, and Xiaohua Zhai. 2023. Tuning Computer Vision Models With Task Rewards. In *40th International Conference on Machine Learning*, Andreas Krause, Emma Brunskill, Kyunghyun Cho, Barbara Engelhardt, Sivan Sabato, and Jonathan Scarlett (Eds.), Vol. 202. 33229–33239.
- Veronique Ventos, Yves Costel, Olivier Teytaud, and Solène Thépaut Ventos. 2017. Boosting a Bridge Artificial Intelligence. In *29th International Conference on Tools with Artificial Intelligence*. 1280–1287.
- Mathurin Videau, Nickolai Knizev, Alessandro Leite, Marc Schoenauer, and Olivier Teytaud. 2023. Interactive Latent Diffusion Model. In *Genetic and Evolutionary Computation Conference*. 586–596.
- Dequan Wang, Evan Shelhamer, Shaoteng Liu, Bruno Olshausen, and Trevor Darrell. 2021. Tent: Fully Test-Time Adaptation by Entropy Minimization. In *International Conference on Learning Representations*.
- Yizao Wang, Jean-Yves Audibert, and Rémi Munos. 2009. Algorithms for Infinitely Many-Armed Bandits. In *Advances in Neural Information Processing Systems 21*, D. Koller, D. Schuurmans, Y. Bengio, and L. Bottou (Eds.). Curran Associates, Inc., 1729–1736.
- Yuxuan Wang, R. J. Skerry-Ryan, Daisy Stanton, Yonghui Wu, Ron J. Weiss, Navdeep Jaitly, Zongheng Yang, Ying Xiao, Zhifeng Chen, Samy Bengio, Quoc V. Le, Yannis Agiomyrgiannakis, Rob Clark, and Rif A. Saurous. 2017. In *INTERSPEECH*, Francisco Lacerda (Ed.). 4006–4010.
- Thomas Weise, Zijun Wu, and Markus Wagner. [n. d.]. An Improved Generic Bet-and-Run Strategy for Speeding Up Stochastic Local Search. *arXiv:1806.08984* ([n. d.]).
- Ronald J. Williams. 1992. Simple Statistical Gradient-Following Algorithms for Connectionist Reinforcement Learning. In *Machine Learning*. 229–256.
- Ke Xian, Chunhua Shen, Zhiguo Cao, Hao Lu, Yang Xiao, Ruibo Li, and Zhenbo Luo. 2018. Monocular Relative Depth Perception with Web Stereo Data Supervision. In *IEEE/CVF Conference on Computer Vision and Pattern Recognition*. 311–320.
- Lin Xu, Frank Hutter, Holger H. Hoos, and Kevin Leyton-Brown. 2008. SATzilla: Portfolio-based Algorithm Selection for SAT. *J. Artif. Int. Res.* 32, 1 (June 2008), 565–606.
- Wei Yin, Xinlong Wang, Chunhua Shen, Yifan Liu, Zhi Tian, Songcen Xu, Changming Sun, and Dou Renyin. 2020. DiverseDepth: Affine-invariant Depth Prediction Using Diverse Data. *arXiv:2002.00569* (2020).
- M. Zameshina, O. Teytaud, Fabien Teytaud, Vlad Hosu, Nathanael Carraz, Laurent Najman, and Markus Wagner. 2022. Fairness in Generative Modeling: Do It Unsupervised!. In *Genetic and Evolutionary Computation Conference Companion*. 320–323.
- Banghua Zhu, Michael Jordan, and Jiantao Jiao. 2023. Principled Reinforcement Learning with Human Feedback from Pairwise or K-wise Comparisons. In *40th International Conference on Machine Learning*, Andreas Krause, Emma Brunskill, Kyunghyun Cho, Barbara Engelhardt, Sivan Sabato, and Jonathan Scarlett (Eds.), Vol. 202. 43037–43067.
- Fuzhen Zhuang, Zhiyuan Qi, Keyu Duan, Dongbo Xi, Yongchun Zhu, Hengshu Zhu, Hui Xiong, and Qing He. 2021. A Comprehensive Survey on Transfer Learning. *Proc. IEEE* 109, 1 (2021), 43–76.
- Shlomo Zilberstein. 1996. Using Anytime Algorithms in Intelligent Systems. *AI Magazine* 17, 3 (1996), 73.

A FULL RESULTS FOR THE AFTERLEARNER / MIDAS EXPERIMENT

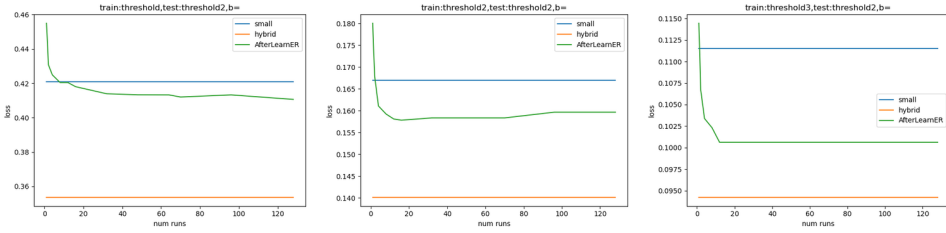
We observe here (i) good performance even with a low budget (total budget < 300 is enough for positive results) (ii) good transfer, in particular when training on Th3. Note that AfterLearnER succeeds in 25 cases out of 27 independent runs, which happens with p-value $2.8e - 6$ under the null hypothesis that the success rate is at most 0.5.

For each budget, there are three loss functions Th1, Th2 and Th3 which can be used in training or in test, hence 9 curves. For 3 of them, train and test use the same loss function: the 6 others are about transfer. The non-transfer cases are also presented in the main text. Fig. 12 considers a budget $b = 1$. Fig. 13 considers a budget $b = 50$. Fig. 14 considers a budget 150. In each figure, the x-axis is the number of runs k . We observe an excellent transfer with b small, which suggests that the good mathematical properties in terms of overfitting (Eq. 2) also indicate a robust transfer.

Testing on Th1, training with Th1, Th2, Th3 respectively:



Testing on Th2, training with Th1, Th2, Th3 respectively:



Testing on Th3, training with Th1, Th2, Th3 respectively:

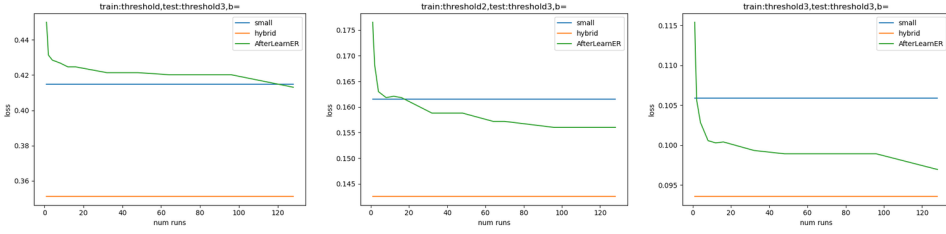
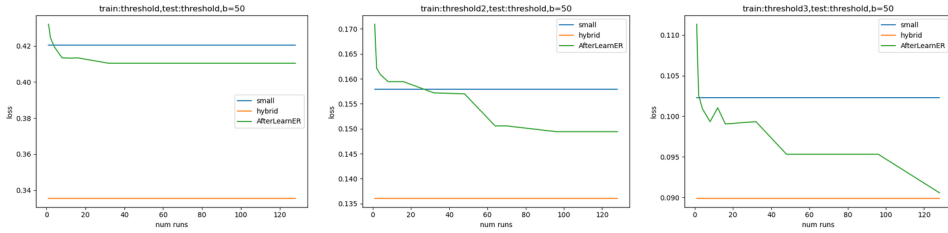
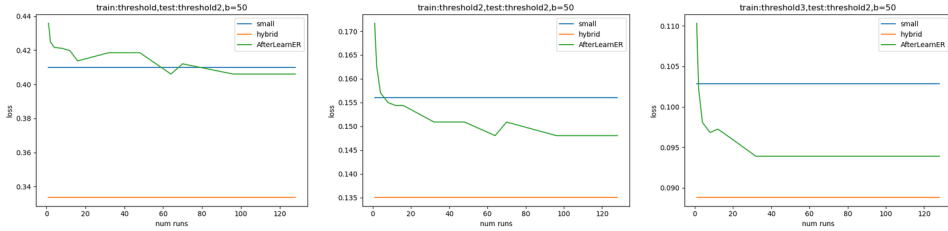


Fig. 12. AfterLearnER applied to MiDaS with budget $B = \{1\}$: with this budget 1, we are actually running random search and already get positive results. We note that with a training on Th3, we get positive results for all tests with $b \times k$ (total number of scalar evaluations provided to AfterLearner) greater than 20: so 20 evaluations is enough for a good transfer to all criteria Th1, Th2, Th3.

Testing on Th1, training with Th1, Th2, Th3 respectively:



Testing on Th2, training with Th1, Th2, Th3 respectively:



Testing on Th3, training with Th1, Th2, Th3 respectively:

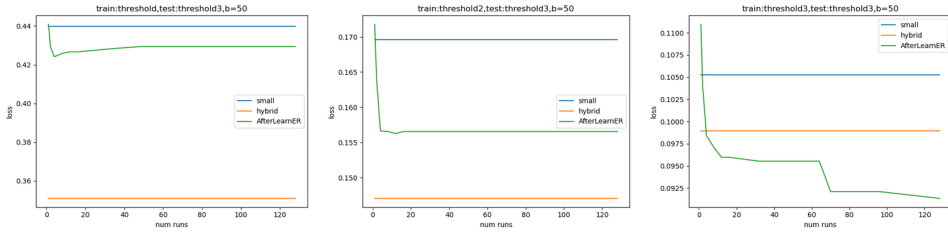
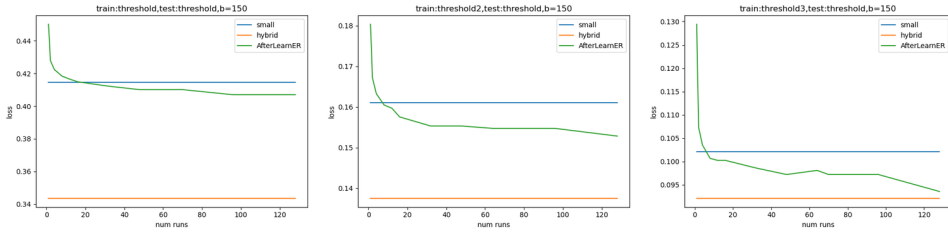
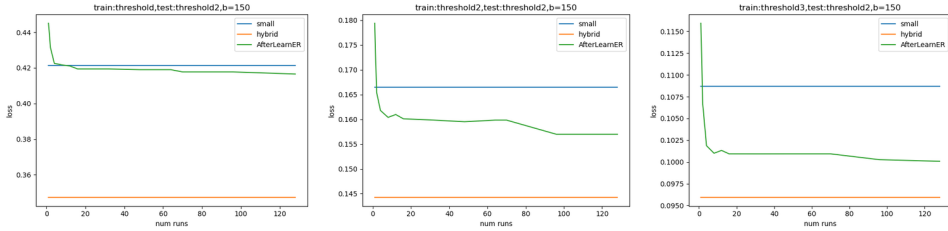


Fig. 13. AfterLearnER applied to MiDaS with budget $B = \{50\}$. Compared to $B = \{1\}$, the number of scalar evaluations needed for beating the baseline is greater, but remains in the hundreds. Th3 remains the best training criterion for good transfer to all 3 criteria Th1,Th2,Th3.

Testing on Th1, training with Th1, Th2, Th3 respectively:



Testing on Th2, training with Th1, Th2, Th3 respectively:



Testing on Th3, training with Th1, Th2, Th3 respectively:

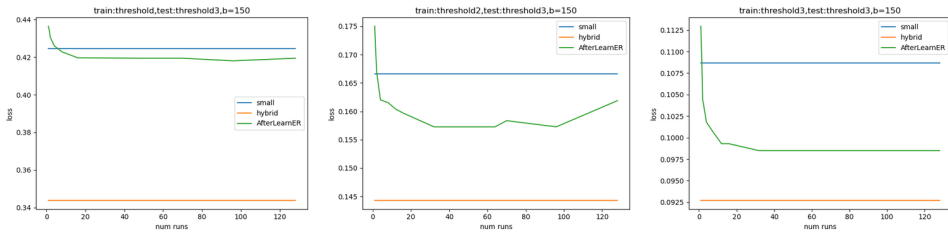


Fig. 14. AfterLearnER applied to MiDaS with budget $B = \{150\}$. Compared to $B = \{1\}$, the number of scalar evaluations needed for beating the baseline is greater, but remains in the hundreds. Th3 remains the best training criterion for good transfer to all 3 criteria Th1,Th2,Th3.

B ASK AND TELL

Algorithm 5 General organization of a parallel asynchronous black-box optimization method o . There is a first-in-first-out (FIFO) pool of pairs $(x, f(x))$ to be computed by the workers. The sequential case corresponds to $P = 1$.

Require: objective function f , number of workers $P \geq 1$, domain D , budget b
 $o.initialize(D, b, P)$ ▷ Initialize o given P , domain D , and budget b

procedure WORKER-TASK(x)
 Compute $f(x)$
 $o.tell(x, f(x))$ ▷ Inform the method o of the performance obtained by the \mathcal{NP} x , no gradient needed

end procedure

for $i \in \{1, \dots, b\}$ **do**
 Wait until there are less than P computations in progress in the FIFO
 Request $x \leftarrow o.ask()$ ($x \in D$) ▷ Choice of \mathcal{N} -parameter to be tested
 Put x in the FIFO of workers tasks

end for

Wait until the FIFO is empty

return $o.recommend()$ ▷ Final returned value

C BLACK-BOX OPTIMIZATION WIZARDS AND NGOPT

After becoming famous in SAT solving [Xu et al. 2008], wizards become important in black-box optimization as well [Awad et al. 2020; Liu et al. 2020; Meunier et al. 2022a; Weise et al. [n. d.]].

Optimization wizards are based on selecting, from characteristics of the domain (dimension, type of variables) and of the optimization run (budget, parallelism), an optimization algorithm or a bet-and-run [Weise et al. [n. d.]] or chaining of several optimization algorithms. NGOpt, an open-source wizard for black-box optimization, is available in [Rapin and Teytaud 2018] and as a PyPi package.

For example, in a continuous setting, with moderate dimension, a large budget, and a sequential optimization context (no parallelism), NGOpt [Meunier et al. 2022a] chooses a chaining of CMA [Hansen and Ostermeier 2003] fastened with a metamodel and followed by Sequential Quadratic Programming [Artelys 2015b].

An example of code involving NGOpt is provided in Appendix D.

D REPRODUCIBILITY

All black-box optimization algorithms are available in [Rapin and Teytaud 2018]. Nevergrad can be installed by cloning <https://github.com/facebookresearch/nevergrad> or by “pip install nevergrad”.

A minimal example of optimization with some optimization methods mentioned above is in Algorithm 6 (without link with deep learning). Algorithm 9 presents an application for the optimization of a single layer of a PyTorch model.

The detailed code to improve EG3D is in Algorithm 8.

A minimal code for running Retrofit on a Pytorch model (all parameters) is Algorithm 7.

E COMPUTATIONAL COST

Algorithm 6 Sample code: Minimal example of black-box optimization.

```
import nevergrad as ng
import numpy as np

def loss(x):
    return np.sum((x - 1.7) ** 2)

# 3 optimization methods in dimension 10, continuous.
optim_ngopt = ng.optimizers.registry["NGOpt"](10, 500)
optim_de = ng.optimizers.registry["DE"](10, 500)
optim_lengler = ng.optimizers.registry["DiscreteLenglerOnePlusOne"](10, 500)

# 1 optimization method for dimension 10, integer values between 1 and 4,
# with 30 parallel evaluations.
array = ng.p.Array(init=np.array([2] * 10), lower=1, upper=4).set_integer_casting()
optim_opo = ng.optimizers.registry["DiscreteOnePlusOne"](array, 500)

# an example with minimize
print(optim_ngopt.minimize(lambda x: loss(x)).value)

# an example with ask and tell
for k in range(50):
    x = optim_de.ask()
    y = loss(x.value)
    optim_de.tell(x, y)

# an example with minimize in a discrete context
print(optim_opo.minimize(loss).value)
```

Algorithm 7 Minimal example of code modifying a Pytorch model for cross-entropy or directly for the classification error. The key point is not minimizing the cross-entropy error (which can be done much faster with gradient-based optimization) but the direct optimization of the success rate.

```
# Our retrofit method:
# less overfitting, more privacy, less poisoning, no fair use issue.
def retrofit(model, epochs, optim_name="NGOpt", cross_entropy=False):
    with torch.no_grad():
        if cross_entropy:
            criterion = nn.CrossEntropyLoss()
        else:
            criterion = binary_accuracy
        d = 0
        # In this version we work on all parameters.
        for name, param in model.named_parameters():
            d += len(param.data.detach().cpu().numpy().flatten())
            #print(d)
    optim = ng.optimizers.registry[optim_name](d, epochs)
    for epoch in range(epochs):
        total_loss = 0
        num = 0
        w = optim.ask()
        set_weights(model, w.value)
        for x, y in train_loader:
            y_scores = model(x)
            if cross_entropy:
                loss = criterion(y_scores, y)
            else:
                loss = criterion(y_scores[:,1], y)
            #loss.backward() not needed here!
            #optimizer.step()
            total_loss += loss.item()
            num += len(y)
        optim.tell(w, total_loss/num)
        #if epoch %
        # print(epoch, total_loss / num)
    set_weights(model, optim.recommend().value)
```

Table 9 presents typical computational costs of AfterLearner for a typical entire run, providing significant improvements compared to the initial DL tool.

F CODE: AFTERLEARNER ONLINE IN THE CASE OF EG3D FOR CAT GENERATION

Algorithm 8 shows the integration of our work in the case of cats generated by EG3D.

G TUNING A PYTORCH MODEL: CODE

Appendix D presents a minimal example of black-box optimization in the general case, in the case of the platform Nevergrad used in all our experiments. In Algorithm 9, we present a few lines of code for optimizing a single layer of a Pytorch model. In Algorithm 7, we provide a function for optimizing all weights of a Pytorch model. The long URL for a small-scale experiment is https://colab.research.google.com/drive/10GujGQp_59SX60kLoGQ5TOKF9Na1ybRM (short URL: <https://tinyurl.com/teloretrofit>): we refer to the reading guide at the top of this link for more details. Additional experiments on residual networks for classifying images are available at <https://colab.research.google.com/drive/1tImBE55mo-NatTlGd-q3nM0mMak4DN92> (short URL <https://tinyurl.com/retrofitresnet>) and for a small scale https://colab.research.google.com/drive/108hV_zNjAqP21C9JIwbIre63Uhx-gGu (short URL <https://tinyurl.com/retrofitresnetsmall>).

Table 9. Computational cost. *Here, the cost is in terms of data collection. **We get positive results even with a very low budget, though greater budgets lead to better results (Figure 3). The online overhead exists only when we modify, online, the latent variables of a GAN for each new generation of images; however, it is typically negligible compared to the generation of images itself.

Application	computational cost	
	Offline comp. cost	Online overhead
Depth sensing (Fig. 2, $k = 10$, $B = 50$)	12h, 10 GPUs	zero
Speech resynthesis (Tab. 4, 1st line)	1 GPU, 2 hours	zero
EG3D (Section 6.2)	200 labelled examples*	negligible
Evol. Interactive GAN (Section 6.1)	selecting 5 batches* out of 30	zero
LDM (offline, Section 6.3)	200 images	negligible
LDM (online, Section 6.4)	negligible	negligible
Doom (Tab. 5)	48 hours, k GPU	zero
Code translation (Section 5.4)	0 to 54 hours**, 0 to thousands of labelled translations	zero

Algorithm 8 The short code at the top of EG3D-cats for getting AfterLearnER on top of it. There is no significant computational overhead, we learn directly from z : we do not generate anything.

```
# Code for modifying a latent vector z, using a list of the
# bad random seeds over the 200 first seeds.
if "afhqcats512-128" in network_pkl:
    Y = [1] * 200 # Seeds 15, 84, 47 are bad for cats.
    bad_latent_z = [15,84,47,30,33,78,4,50,49,
                    56,11,17, 36,85,59,16,63,81,25,39, 87,45,41,58,60,68,46,38]
    bad_latent_z += [130,113,146,107,143,
                    175,158,192,121, 110,181,186,170,120,163,193,155,
                    144,148,191,141, 105,187,183,174,
                    129,117,100,157,166,194,198,138, 156,168,114,127,103,109]
if "ffhqrebalanced512-64" in network_pkl:
    Y = [1] * 200
    bad_latent_z = [27,14,88,42,37,25,73, 53,40,17,45,92,
                    50,3,84,29,12,31,98,72,51,46,57,16,13,33,
                    43,69,60,74, 77,75,41,89,39,87,68,67,56,
                    35,26,9,23,7,38,20,63,55, 28,36,8,6,64]
    bad_latent_z += [132,145,194,187,119,169, 137,176,185, 147,111,139,171,
                    101,161,116,115,155,175,118,112,144,172,
                    198,124,181, 129,117,189,108,174,138,121,143,
                    156,130,146,179,140,153,136,168,131,180,110, 109,199,100]
for p in bad_latent_z:
    Y[p] = 0
# Random generation
X = [list(np.random.RandomState(i).randn(1, G.z_dim)[0])
      for i in range(len(Y))]
# Learning with Scikit-Learn.
from sklearn import tree
clf = tree.DecisionTreeClassifier()
print(len(X), len(Y), len(X[0]))
clf = clf.fit(X, Y)
# Optimization with Nevergrad: modify bad cats.
z = np.random.RandomState(seed).randn(1, G.z_dim)
import nevergrad as ng
epsilon = 0.01
def loss(x):
    assert len(x) == G.z_dim
    return clf.predict_proba(
        [list(z[0] + epsilon * x)])[0][0]
nevergrad_optimizer = ng.optimizers.NGOpt(G.z_dim, 10000)
for nevergrad_iteration in range(1, 10000):
    x = nevergrad_optimizer.ask()
    l = loss(x.value)
    if l < 1e-5:
        break
    else:
        nevergrad_optimizer.tell(x, l)
print(f"Success in {nevergrad_iteration} iterations")
z[0] += epsilon * nevergrad_optimizer.recommend().value
```

Algorithm 9 Python code for tuning a single layer of a Pytorch model (we refer to Algorithm 7 for a more general case). In this example, we focus on the last layer.

```
import nevergrad as ng
# Here you need to load your Python model.
Todo.
# Get a good initial value:
with torch.no_grad():
    w0 = my_model.output.weight.data.detach().cpu().numpy
# w0.shape can then be used for initializing an array ng.p.Array(shape=w0.shape):
my_optim = ng.optimizers.DiscreteLenglerOnePlusOne(
    ng.p.Array(shape=w0.shape), budget=500)
# w0 can then be used in optim.suggest().
my_optim.suggest(w0)
# Modify the value so that it becomes w:
for i in range(my_optim.budget):
    w = my_optim.ask()
    with torch.no_grad():
        my_model.output.weight.data.copy_(torch.tensor(w.value))
    loss = Todo
    #After computing the loss loss (e.g. loss=-accuracy):
    my_optim.tell(w, loss)
# The optimization is over:
# we put the recommended w
# in the pytorch model.
w = my_optim.recommend()
with torch.no_grad():
    my_model.output.weight.data.copy_(torch.tensor(w.value))
# You might save your model here.
Todo.
```
